20.

Evaluation of Wind Statistics and Energy Resources in Southern RI Coastal Waters

A. Grilli, M. L. Spaulding, A. Crosby, and R. Sharma
Ocean Engineering
University of Rhode Island
Narragansett, RI 02882

October 15, 2010

Executive Summary

The focus of the present study is to characterize the wind resources in southern RI coastal waters based on model simulations performed by AWS TrueWinds and historical observations and hindcasts in the study area. Both model predictions and observations show wind speeds increasing with distance offshore, with wind power approximately doubling between the RI shoreline and Block Island. Westerly winds are dominant in the study area with NW dominant west of Block Island and W and SW winds dominant to the east and near shore. Block Island Sound is in the lee for winds from the WSW to W from Long Island while Buzzards Bay and Nantucket Sound are in the lee of the main land for winds from the NW. Winds in the vicinity of Block Island are impacted by the topography and land cover on the island. Offshore buoy observations in coastal waters show a dominant NW to NE pattern off Block Island and a W dominance for observations in RI Sound for the observation period from Oct 2009 to May 2010. The northwesterly to westerly dominance is consistent with equivalent winter observation periods.

Table of Contents

List of Figures

List of Tables

List of Appendices

Appendix A : Wind frequency and power density (seasonal and annual) roses and Weibull distribution fits for selected stations in the SAMP study area.

For this appendix material, see Appendix A of Spaulding, et al., 2010, "Wind Resource Assesment in the Vicinity of a Small, Low Relief Coastal Island" – this report.

Abstract

The focus of the present study is to characterize the wind resources in southern RI coastal waters based on model simulations performed by AWS TrueWinds and historical observations and hindcasts in the study area. Both model predictions and observations show wind speeds increasing with distance offshore, with wind power approximately doubling between the RI shoreline and Block Island. Westerly winds are dominant in the study area with NW dominant west of Block Island and W and SW winds dominant to the east and near shore. Block Island Sound is in the lee for winds from the WSW to W from Long Island while Buzzards Bay and Nantucket Sound are in the lee of the main land for winds from the NW. Winds in the vicinity of Block Island are impacted by the topography and land cover on the island. Offshore buoy observations in coastal waters show a dominant NW to NE pattern off Block Island and a W dominance for observations in RI Sound for the observation period from Oct 2009 to May 2010. The northwesterly to westerly dominance is consistent with equivalent winter observation periods.

1.Background

In 2006, the RI Office of Energy Resources contracted with Applied Technology Management (ATM) to assess to whether wind energy could meet the State's renewable energy goals of 50 MW by 2016. Given a typical wind capacity factor, this would require an installed capacity of 450 MW. ATM (2007a,b) concluded that the goal could be met but would require development of offshore wind resources. Restricting their attention to water depths less than 23 m (75 ft), where mono-pile structures are feasible, they estimate that 95% of the available wind energy resource in RI is from offshore waters. The study also identified sites for potential offshore wind development that could either individually or collectively meet the state's renewable energy goal. In performing their assessment, ATM used data provided by AWS True Winds (Brower, 2007) to estimate wind energy resources. AWS True Winds provided annual mean wind speeds at 30, 50, 70, and 100 m and mean wind power at 50 m. The data were generated by AWS TrueWind's MesoMap meteorological modeling system and included the southern New England states (Rhode Island, Massachusetts, and Connecticut) and adjacent coastal waters. The data were provided on a 200 m by 200 m resolution grid. AWS validated the model predictions by comparison to 33 stations located in southern New England, only three of which were in coastal waters.. The model root mean square error was reported to be 4% based on comparisons of annual mean wind speeds at an elevation of 65 m. Observed data at individual comparison sites were extrapolated from the observation height to the 65 m reference level using frictional local scaling. The vast majority of sites used for validation were on land. There were only three validation sites in RI (Providence, Pt Judith and Block Island) and none in RI coastal waters. Buzzards Bay was the only validation site in southern New England coastal waters. National Renewable Energy Laboratory (NREL) reviewed the maps and found that they under predicted the winds in the area around Boston Harbor, based on a comparison to observations at Logan Airport, Boston Harbor, and other nearby stations. AWS True Winds adjusted the maps (5% increase in wind speed) to address this problem.

Anticipating the use of these data to define the wind energy resource as part of the marine spatial planning undertaken by the RI Ocean Special Area Management Plan (SAMP) and given the lack of validation of the estimates for SAMP study area (Figure 1) an independent analysis was performed and is the focus of the present report. This effort consisted of (1) obtaining AWS TrueWinds data from ATM, (2) identifying and collecting historical wind observations for all

sites in the SAMP study area or immediately adjacent to it, and (4) then comparing mean annual estimates from these observation stations to the model data product. Additional statistical analyses were performed on the observed data to support other SAMP study elements.

In related work, Spaulding et al (2010b and c) summarize observations in the immediate vicinity of Block Island. Spaulding et al 2010b use a template scaling method based on high resolution meteorological model (RAMS) predictions for discrete wind directions and a wind frequency rose to estimate mean annual wind speed and power fields south of the island. Spaulding et al (2010c) use the same meteorological model to predict wind speeds and power in the same study area to hindcast the winds from October 2009 to February 2010. Predictions are compared to observations from an offshore buoy, a meteorological tower located on Block Island, at the Block Island Airport (KBID) and from Weatherflow's Block Island Jetty site.

2. The Data

Presented below is a summary of the data available to perform the analysis. An overview of the AWS True Winds model predicted data is presented first followed by the available observations. Details on each data set are provided in Table 1.

AWS True Winds Data

The modeling methodology used to generate the wind maps and their validation is presented in Brower (2007). Figure 2a to d show contour plots of the AWS TrueWinds mean annual wind speed maps at 30, 50, 70, and 100 m, respectively. The data at all vertical levels show a clear increase in wind speed as a function of distance offshore. The wind speeds are also observed to increase with height above the sea surface.

Assuming a neutrally stable atmosphere, on average, the wind speeds at 30 and 100 m were used to estimate the friction or shear coefficient, where wind speeds are U_1 at height h_1 and U_2 at height h_2, and r is the friction or shear coefficient (Hsu et al, 1994).

$$U_2 = U_1 \left[\frac{h_2}{h_1} \right]^r \qquad (1)$$

Based on this analysis the friction coefficient for the offshore study area for the mean annual wind speed was approximately constant at 0.134. For near shore sites the friction coefficient increased to 0.16 and higher reflecting the proximity of the coast and the greater roughness on the main land. The standard reference value used for a neutrally stable atmosphere is 1/7 or 0.143.

Observations

An in-depth review was performed to identify any data sets that might be used to compare to model predictions. The criterion were that the data had to be from a recognized source with suitable quality control and the wind observation period should be at least 1 yr, and preferably much longer, ideally 6 years(see analysis to follow).. A summary of the data sets identified in this process are given below. The locations of the observation stations are provided in Figure 3a for the WIS stations and 3b for the rest.

Five data sources and associated data sets were identified: US Army Corp of Engineers, Wave Information Study (WIS), Martha's Vineyard Coastal Observatory, WeatherFlow, NOAA National Data Buoy Center (NBDC), and Department of Energy (DOE). The data sets including the station number/location, period, recording height, frequency of observation, and type (measured or hindcast) are provided in Table 1. Links to the sites from which the data were obtained are provided at the bottom of the table, if the data was available on line. Additional wind observations are currently being collected from two offshore buoys, one immediately south of Block Island, and one NNE of Cox's Ledge (October 1, 2009 to present). Measurements are also being made at four vertical levels from a meteorological tower on the coast of Block Island, nearby the western entrance to Great Salt Pond (August 1, 2009 to present). None of these measurements are discussed here because of their short record lengths. Selected analyses of the data are provided in Appendix A.

Army Corp of Engineers Wave Information Studies (WIS)

The US Army Corp performed a 20 yr hindcast (1980-1999) of the wind and wave conditions for a number of sites located along the southern boundary of the study area as part of the Wave Information Study (WIS). The locations of the southern New England hindcast sites are shown in Figure 3a. The sites of primary interest in this investigation are 74 to 79, 95, 100,

and 101, located in a coast parallel configuration. Time series data are available via the internet at each location over the 20 yr hindcast period. Winds are estimated at 10 m elevation. The hindcast were made primarily validated with data from NOAA NDBC offshore observations (Stations 44004, 44008, 440017, 440018, and 44025).

Martha's Vineyard Coastal Observatory (MVCO)

Woods Hole Oceanographic Institution (WHOI) installed the MVCO to perform fundamental research in coastal meteorology. The meteorological tower from which the observations were made is in close proximity to the southern coast of Martha's Vineyard.

WeatherFlow

WeatherFlow is a private firm that operates a network of meteorological observation towers in the littoral zone, throughout the United States. In particular, several dozen sites are located in Southeast New England, with exact locations ranging from 0.2 km inland, to several sites located on stationary navigational aids an distances averaging 0.2 to 0.4 km off shore.

The data is distributed through their IWindSurf web site. Historical data (not normally available) for the Pt Judith, Rose Island, Half Way Rock and Block Island Jetty (western entrance to Great Salt Pond) stations , were provided by WeatherFlow Inc. (J. Titlow, personal communication).

NOAA/ NDBC

NOAA/NBDC operates two meteorological observation sites close to the SAMP site, one at the entrance to Buzzards Bay (BUZM3) and the second a 3 m discus buoy (44017) located off the southern coast of Long Island (40.691 N 72.046 W). These two are the closest NOAA/NDBC buoys to the study area. While data from BUZM3 are available from the mid 1980s to present, the data prior to 1999 had substantial discontinuities and therefore was not used.

Department of Energy (DOE)

DOE made wind measurements at a site just south of Great Salt Pond as part of a feasibility study to investigate the siting of a wind turbine on the island (Renne et al, 1982). This measurement program was unusual in that measurements were made at two locations in the vertical (9.1 and 45.7 m). The site is located on a hill top in rolling grass land.

Other

Wind observations were obtained under an educational institution license agreement from the meteorological tower established for the Cape Wind project on Horseshoe Shoals in Nantucket Sound, MA (http://capewind.whgrp.com/). This data set is not publically available. An analysis of the data was performed found to be consistent with the analyses that follow but Cape Wind would not allow its release at the time of this report.

Wind data is available from the Automated Weather Observation Stations (AWOS) at Block Island Airport (KBID) from 1997 to present. An analysis was performed of the data and showed a strong SW dominance. A decision was made not to use this data in the present analysis for the following reasons: (1) the site is on land with significant tree cover and topographic relief immediately to the W and NW of the observation site. (Model simulations by Spaulding et al (2010 b, c) show very large shear, 0.45, year round in the vicinity of the airport), (2) the AWOS was located within 50 m of the airport terminal (height 12 m)(terminal to west of AWOS) until a new terminal was constructed in 2009. The short distance between the AWOS and the terminal building was in violation of FAA siting standards for AWOSs.

3. Data Analysis

Wind statistics

Height adjustments and friction coefficients

The data provided by AWS TrueWinds are annual mean values. Access to the underlying time series data or frequency distributions either by speed or direction was not available. Given this situation the first step in the analysis was to determine the mean wind speeds for each observation record at the observation height. These values were then adjusted to a standard reference height of 65 m using Equation 1. The vertical reference is the same as used by Brower (2007) in his validation of the AWS TrueWinds predictions. A friction coefficient of 0.1 was used to be consistent with the value employed by ATM (2007a). Table 2 summarizes the minimum, maximum, mean, median, skewness, and kurtosis for the observations at each station. Focusing on the means, it is noted that values for the various WIS sites are remarkably similar, with mean values of 8.15 m/sec. For locations closer to land (Pt Judith, MVCO) the means are lower at 6.4 to 7 m/sec, while at the BUZM3 site they are 8.5 m/sec., comparable to the WIS

sites. Inside Narragansett Bay (Rose Island and Half Way Rock) the mean values decrease to 6.4 to 6.6 m/sec.

To assess the sensitivity of the mean values to the friction coefficient estimates were made at 24.5, 65, and 80 m elevations. The 24.5 m elevation was selected because it is the height of observations at the BUZM3 station (the most central, longest duration, and highest elevation observation in the study area), 65 m because it was used by Brower for validation, and 80 m since this is the projected hub height of the proposed wind power development in RI waters. Two values of friction coefficient were employed, 0.1 as in ATM (2007a) and 1/7 = 0.143, as this is a typical value (Hsu et al, 1994) and consistent with the AWS True Winds data for offshore areas (Figure 4). Table 2 presents the results of this analysis. The larger the value of the friction coefficient the higher the wind speed at a given elevation. At 65 m the mean wind speed at the offshore sites increases about 0.4 to 0.5 m/sec as the friction coefficient increased from 0.1 to 0.143.

Figure 5 shows a comparison of the AWS True Wind estimates at each of the stations provided in Table 1 that are within the SAMP area or adjacent to it (BUZM3, MVCO). Values are provided at the 30 m elevation since this was the closest elevation of the AWS TrueWinds data to the vertical location of the observations. The data clearly show the gradient in wind speed with distance from shore; low values near the coast (Pt Judith (PJ)and MVCO) and higher values offshore (BB, WIS).

The probability distribution of the differences between the observations and predictions was estimated and found to be normally distributed (Figure 6) with a mean value of 0.17 m/s and a standard deviation of 0.14 m/s. The predicted AWS wind speed, at maximum, overestimates the observations by 0.44 m/s and, at minimum, underestimates measurements by 0.10 m/s (at the 95 % confidence interval). The AWS estimates are slightly higher than the observed values. Brower (2007) estimated the root mean square error between predicted and observed/extrapolated winds as 0.5 m/sec or 6.6 % for the 32 stations where comparisons were made. He estimated a 0.1 m/sec bias with the predictions lower than the observations. The present results are generally consistent with his analysis

One area of concern in analyzing the data is the impact of wind observation record length on estimates of the mean values. The observation record lengths vary substantially from 2 to 20 yrs (Table 1). The sensitivity of the mean wind speed value to the record length was performed for all WIS stations and BUZM3. These were selected since they have the longest hindcast and observed records (20 and 7 yrs, respectively) in the study area. Results were similar for all WIS stations therefore only the values from Station 101 are presented. The data were analyzed at a 10 m elevation for WIS 101 and 23.5 m for BUZM3. These are the original elevations at which the data were reported.

Annual and cumulative annual (from the beginning of the record) mean wind speed were estimated from the time series and are shown in Figure 7 and 8 for WIS101 and BUZM3, respectively. A review of the data shows that the annual variability is on the order of 0.4 m/sec. at both sites. The year to year variability can be as large as 0.8 m/sec at WIS101 and 1 m/sec at BUZM3. The averaging inherent in a cumulative analysis significantly reduces the variability with time. At WIS 101, approximately 6 yrs of data are required for the cumulative value to reach its long term mean. The data actually show a slight downward trend with time, but an analysis shows the trend is not statistically significant. Cumulating the values reduces the variability for BUZM3 but the time to reach the long term mean is not clear. The role that climate change, El Nino, and other long term processes play is influencing the long term trend is also not clear.

An identical cumulative analysis, except backward in time, was performed for WIS 101. The results of both the forward and backward in time cumulative analyses are shown in Figure 9. Once again the 6 yr averaging time to achieve steady state conditions is shown.

Wind speed probability distributions

To provide additional insight into the winds in the study area, Weibull distributions were fit to the observation data. These distribution functions allow estimates of the wind power generation to be made and highlight the differences between the median and mean values observed in the analysis. Weibull distributions have two fit parameters, c (magnitude) and k (shape) that are varied to fit the data. These values were determined by a least squares fit for all observation stations. The results are reported in Table 2 (last two columns). Figure 10 shows a

sample of the curve fit at 65 m elevation to WIS 74(upper panel) and BUZM3(lower panel), respectively. The values for c are very similar (c = 9.3) and k is close to 2 for the WIS and BUZM3 stations. The k values for the near shore stations, MVCO and Pt Judith, are comparable to the offshore stations. The c values (7 to 8) are substantially lower; consistent with the lower wind speeds at these locations (Table 2). For comparison ATM(2007a) estimated k = 2 and c = 7.22 (6.5 m/sec winds) and 7.78 (7 m/sec winds) for on shore sites. Grilli and Spaulding (2010) present a more comprehensive analysis using Weibull based distribution analysis. This paper shows how the shape and amplitude parameter vary with proximity to land. The paper also estimates the power production potential in the area using a Weibull based analysis.

Extreme wind speed analysis

An analysis was performed to estimate the mean and upper 95% percentile, once in 20, 50, 75, and 100 yr return period wind speeds as a function of wind direction at WIS 101. These estimates are critical to determining environmental loading on the wind turbine support structures. The estimates were determined by a Gumbel distribution fit to the maximum monthly mean wind speed data. Thirty (30) degree bins were used, centered on 90, 120, 150, 180, 210, and 240 degrees. The meteorological convention for wind direction was used. The results are reported in Table 4 for both mean and upper 95 % confidence limit values. The wind speed increases with return period and the greatest exposure is from the north. The mean and upper 95% confidence limit maximum winds for 100 yr return period are 31 and 34 m/sec, respectively

Wind and wind power directional distribution

Wind speed and power roses were prepared for all stations located in the SAMP study area and are shown in Figure 11 and 12, respectively. The figures show the directional values by speed or power for each direction. Figure 13 shows the average wind power by directions. This value is calculated by frequency weighting the value of power from each direction. (Appendix A provides wind speed, power density and average power roses for all sites.) The large scale trends show that the wind speeds and power roses are dominated by westerly winds. West of Block Island and offshore NW winds dominate, while east of the island and closer to show the winds are more westerly and southwesterly.

To assist in interpreting the wind roses Figures 14 (October 30, 2008- NW), 15 (July 8, 2008-SW), and 16 (September 24, 2008 – NE) show hindcast wind speed contours from a nested high resolution meteorological model applied to the SAMP study area. Spaulding et al (2010c) describe the model application and validation with observations in detail. These simulations represent typical winter (NW), summer (SW) and NE (storm conditions). All the simulations show that the wind speed increases with distance offshore reaching maximum values south of Block Island. The rate of increase is greatest for shore parallel winds (SW) and lowest for offshore winds (NW). The lee effect of Long Island is clearly evident in western Block Island Sound. At locations close to the shoreline the wind speeds from the NW are substantially reduced due to flow over land while those from the SW are unimpeded since the wind flow is over water; the closer to land the greater the effect. This analysis shows that the available wind power increases substantially with distance offshore. South of Block Island the increase with distance offshore is greatly diminished.

Wind and wind power directional distribution

Wind data were analyzed at WIS 101 at 80m to determine the directional distribution for all observed winds and for winds that are appropriate for extraction of energy using current wind turbine technology. This site was selected as it representative of offshore waters. "Extractable" is defined as wind speeds above 3.5 m/sec (cut-in speed of the wind turbine) but below 27 m/sec (cut out speed of the turbine). These values depend on the characteristics of the specific wind turbine but the limits given above are reasonable for the current generation of technology. Figure 17 shows a wind rose giving the number of observations (hourly intervals over 20 yrs) by direction for all winds (left panel) and extractable winds (right panel). Note the two figures have difference scales. Figure 18 shows the probability of occurrence for both cases. Both figures show that winds are primarily from the west northwest and secondarily from the west and south west. Winds from the east are substantially less frequent. The extractable winds show the same pattern as the all winds case but at 90%.

Estimates of mean wind power by direction, for all and extractable wind cases, are shown in Figure 19. This value is calculated by taking the average of wind power for each 30 degree direction segment. Figure 20 shows seasonal plots of the all wind case. Figure 21 provides a histogram of the data show in Figure 19, top panel all winds and bottom panel extractable winds.

The power is largest (1.3 kW/m^2) when the winds are from the west northwest and still substantial for winds from the north (1 kW/m^2). Mean wind power is much lower (0.6 kW/m^2) for winds from the southwest to the east. The all and extractable wind cases show similar directional distributions, but the extractable power is slightly lower. The mean, averaged over all directions, is 841 kW/m^2 for the all case and 825 kW/m^2 for the extractable case. Figure 20 clearly shows that winter winds have the highest energy levels (1.9 kW/m^2), fall and spring intermediate levels (1.2 kW/m^2), and summer the lowest levels (3.8 kW/m^2). The power levels are largest from the northwest for fall, winter and spring winds and from the north to northeast for summer winds. Wind power in the winter from all directions exceeds those from every other season

Figure 21 and 22 show corresponding plots for the directional average all and extractable wind cases. Average here is defined as the weighting of the mean power resource by frequency of occurrence (Figure 12). Given the dominance of the stronger westerly winds the average wind power is highest from the west to northwest (160 kW/m^2) and lowest from the east and southeast (2o kW/m^2). Summing the average wind power over all directions gives 841 kW/m^2 for the all wind case and 825 kW/m^2 for the extractable case; the same values as the mean for the mean wind power results.

Estimates of the spatial distribution of the mean wind power were next made on a 100 m by 100 m grid covering the SAMP study area (Figure 1). To make this estimate a Weibull distribution was assumed at each of the grid locations in the study area. Based on the analyses presented in Table 2, the k value for the distribution was observed to be close to 2. For this special case, the Weibull distribution reduces to a Rayleigh distribution. For Rayleigh distributed winds c = $\boldsymbol{U}$/0.886, where $\boldsymbol{U}$ is the mean wind speed at a given location. More details are given on the spatial distribution of the shape parameter in Grilli and Spaulding (2010), but in this approach, the shape coefficient is assumed to be equal to 2 and the distribution is therefore a simple function of the mean wind speed. At each grid cell, the Weibull parameters (c=f(U),k=2) are used to generate a wind speed distribution; 10,0000 wind speed vectors are randomly drawn from each distribution and converted into power. The mean power value is then calculated at each grid cell . Power was alternatively calculated analytically from the Weibull parameters and results are comparable. The choice of the Monte Carlo method is driven by its flexibility to

introduce the concepts of cut-in, cut –out, rated speed, although not use in this particular analysis. A detail analysis of the expected power spatial distribution is presented in a more comprehensive approach by Grilli and Spaulding (2010).The results of the analysis are presented in the form of contour plots of mean wind power. Figure 23 and 24 show the mean wind power contours for the study area for the all and extractable wind cases, respectively. These assume that the mean wind speed estimates from AWS are accurate. Both figures show the mean wind power increasing with distance offshore, consistent with the wind speed contours. The power levels just south of Block Island are 900 W/m^2, twice their value along the southern RI coast line (450 W/m^2) for the all wind case. The values for the extractable winds are about 10% lower than the all winds case. The spatial structure is exactly the same.

It has been shown earlier in the report that the winds from AWS are biased high (0.17 m/sec) from the observed winds. The spatial analysis was repeated using the AWS adjusted for the bias. These results are provided in Figures 20 and 21 for the all and extractable case, respectively. Not surprisingly the patterns are comparable to all winds case however the magnitudes are reduced by approximately 20 W/m^2.

Recent observations

As part of the SAMP investigation three new sets or data have become available. The SAMP project deployed two buoys that are collecting data on wind speed and direction. The data is being collected at an elevation of 4 m. The stations are located (Figure 27) immediately south of Block Island (MDS) and NNE of Cox's ledge at MDF. In addition data is being collected at AWS meteorological tower located at the western entrance to Great Salt Pond on Block Island. Measurements are being made at 9.9, 32, 47.6, and 57.4 m. Data from the MDS and MDF are available from October 1, 2010 to present while data from AWS Met site from August 2009 to present.

Figure 28 shows the observed wind speed time series from the beginning of the recording period through mid February. The mean speeds are 8.01 m/sec at AWS Met, 8.35 m/sec at MDS and 7.95 m/sec at MDF. Wind speed frequency roses are shown in Figure 29 and power roses in Figure 30. The roses are strongly dominated by winds from the NW and secondarily from the NE at AWS Met and MDS. Winds from the westerly direction are dominant at MDF. This basic

pattern is consistent for winter winds and the transition for NW to W-SW dominance noted earlier.

Shear estimates were made from the AWS Met site using data at each of the various levels. The results showed that the values decreased from 0.18 in August to 0.08 in November and remained in the range of 0.06 to 0.07 through February 2010. The shear was approximately the same no matter which vertical levels were used to perform the analysis. The shear for the winter season at AWS Met is consistent with oceanic conditions and stable transitioning to an unstable atmosphere from late summer to winter. The impact of topographic relief and roughness is minimal, as might be expected based on the station's location near the shoreline at the entrance to Great Salt Pond.

4. Conclusions

A comparison was performed between the AWS True Wind predictions of annual mean wind speeds (200 m by 200 m grid) to all wind data publically available in the SAMP study area and those from nearby stations. The principal data sources, with record lengths ranging in duration from 2 to 20 yrs, were US Army Corp WIS, WeatherFlow, Martha's Vineyard Coastal Observatory, and NOAA/NBDC stations. Comparisons were made at an elevation of 65 m. Data sets were adjusted to this elevation using standard frictional scaling. The analysis showed that the wind speeds from the model and observations were in good agreement with the observations (mean difference of 0.17 m/sec and standard deviation of 0.14 m/sec). The mean annual wind speeds were 6.8 m/sec at coastal stations and 8.1 m/sec at offshore stations. Viewed in terms of an onshore-offshore transect, observations were only available very close to the shore and at a distance of about 40 km offshore, hence only two locations. Additional observations at intermediate and greater distances will be required to characterize the width of the coastal boundary layer.

Estimates of the frictional coefficient, based on the AWS True Winds data, were made at the observation sites and show that the value is constant for offshore waters (0.128) but increased substantially at near coastal stations (0.16 to 0.19). It was impossible to verify these estimates since wind observations were only available at one height at each station. The increased frictional resistance at very near coastal stations is consistent with increased roughness over land.

The annual variability of the mean wind speed was investigated at WIS 101 (20 yrs) and BUZM3 (7 yrs) and showed typical year to year variations of 0.4 m/sec, with maximum differences on the order of 0.8 to 1 m/sec. A sensitivity study was performed on estimates of the annual mean value based on length of record used in the averaging. The analysis showed that 6 years of data were required at WIS101. No conclusion could be drawn at BUZM3 however since the record was only 7 years in length.

Wind observations at all stations were fit with a Weibull probability distribution function. The shape parameter, c, was approximately 2 for all stations. The amplitude parameter, k, was 9.3 at offshore sites but decreased to about 7 at near shore locations. This result is consistent with the gradient of wind speeds with distance offshore.

An extreme analysis of the once in 20, 50, 75, and 100 year return period wind speeds by direction was performed. Mean and upper 95% percentile values were estimated by 30 degree direction bins. The maximum mean and upper 95% values for the once in 100 year event were 31 and 34 m/sec from the north.

A directional analysis of the wind speed and power was performed for WIS site 101 at 80 m. The analysis shows that the winds from the northwest to southwest have the highest frequency of occurrence, with the power being from westerly to northwesterly winds. Wind power is substantially larger in the winter months, intermediate in spring and fall and smallest during the summary. The analysis was performed for all and extractable. The patterns are exactly the same but the magnitude of the later is about 90% of the former.

Using a Weibull distribution and the mean AWS wind speeds contour maps of wind power were generated for the study area. The wind power contours are shoreline parallel and increase with distance offshore from 450 kW/m^2 to 900 kW/m^2. The analysis was performed again correcting the mean AWS wind speeds for a positive bias. The power levels generally decreased about 20 kW/m^2 when compared to AWS based estimates.

Recent measurements from AWS Met, MDS and MDF show a NW followed by NE dominant pattern for the first two and W dominance for MDF for the October 2009 to present measurement period. The pattern is consistent with historical data in the study and the transition

for NW to W dominance as one moves eastward. The shear coefficient at AWS Met was low (0.08) typical of unstable winter winds.

References

ATM, 2007a. RI WINDS Phase I, Wind Energy Siting Study, prepared for RI Office of Energy Resources, Providence, RI, April 2007.

ATM, 2007b. RI WINDS Summary Report, prepared for RI Office of Energy Resources, Providence, RI, September 2007.

Brower, M., 2007. Wind resource maps of Southern New England, prepared by True Wind Solutions, LLC, 10 p.

Grilli, A and M. L. Spaulding, 2010. Estimation of offshore wind power resources based on Weibull distribution in Rhode Island coastal and offshore waters, Ocean Engineering, University of Rhode Island, Narragansett, RI.

Grilli, A., M. L. Spaulding, C. Damon, and R. Sharma, 2010. High Resolution Application of the Technology Development Index (TDI) in State Waters South of Block Island, Ocean Engineering, University of Rhode Island, Narragansett, RI.

Hsu, S. A., Eric A. Meindl, and David B. Gilhousen, 1994. Determining the power-law wind-profile exponent under near-neutral stability conditions at sea, Applied Meteorology, Vol. 33, No. 6, June 1994

Renne, D. S., W. F. Sandusky, and D. L. Hadley, 1982. Meteorological field measurements at potential and actual wind turbine sites, US Department of Energy, Pacific Northwest Laboratory, Richland, WA, PNL -4431, UC-60, September 1982.

Spaulding, M. L., A. Grilli, C. Damon, and G. Fugate, 2010a. Application of technology development index and principal component analysis and cluster methods to ocean renewable energy facility siting, Marine Technology Society, Special Issue on Marine Technology for Offshore Wind, Vol. 44, No 1, January/ February 2010, pg 8-23.
Format: Paper, Status: Published

Spaulding, M. L, R. Sharma, A. Grilli, M. Bell, A. Crosby and Lauren Decker, 2010b. Wind resource assessment in the vicinity of a small, low relief coastal island, Ocean Engineering, University of Rhode Island, Narragansett, RI.

Spaulding, M. L. ,M. Bell, J. Titlow, A. Grilli, R. Sharma, L. Decker and D. Mendelsohn, 2010c. Meteorological model based wind resource assessment in the vicinity of Block Island, Ocean Engineering, University of Rhode Island, Narragansett, RI

Table 1 Wind observations used in analysis

Data Name	Period	Recording Height(m)	Frequency (hrs)	Type
US Army Corp Engineers WIS Stations 74-79, 89, 95, 100, 101				
	1980-1999	10	1	Hindcast
Martha's Vineyard Coastal Observatory (MVCO)				
	2001-2008 (data missing 2005-2008)	12.5	0.33	Measured
WeatherFlow				
Pt. Judith	2005-2007	22.3	1	Measured
Rose Island	2005-2007	10.7	1	Measured
Half-Way Rock	2005-2007	8.23	1	Measured
NOAA/NDBC				
BUZM3	1999-2007	24.8	0.17	Measured
Buoy 44017	2002-2007	5	0.17	Measured

Data Sources

WIS	http://www.frf.usace.army.mil/cgi-bin/wis/atl/atl_main.html
MVCO	http://mvcodata.whoi.edu/cgi-bin/mvco/mvco.cgi
WeatherFlow	http://www.weatherflow.com/
NOAA/NBDC	http://www.ndbc.noaa.gov/

Table 2 Wind speed statistics for WIS, Martha's Vineyard Coastal Observatory, WeatherFlow, and NOAA/NDBC data.

Descriptive statistics wind (m/s) at 65m; wind at 65m = wind @ h0 *(65/H0)^alpha; where alpha = friction coefficient = 0.1.

Station WIS	Period	Min m/s	Max m/s	Mean m/s	Median m/s	Skewness	Kurtosis	Weibull c Magnitude parameter	Weibull k Shape parameter
#74	1980-1999	0.24	42.57	8.23	7.6	0.77	0.46	9.31	2.02
#75		0.24	38.35	8.2	7.48	0.77	0.46	9.19	2.03
#76		0.24	39.19	8.16	7.48	0.77	0.45	9.27	2.03
#77		0.24	41.12	8.13	7.48	0.78	0.46	9.23	2.03
#78		0.24	40.28	8.12	7.48	0.77	0.44	9.23	2.03
#79		0.36	39.43	8.12	7.48	0.76	0.42	9.27	2.04
#89		0.24	32.2	8.15	7.48	0.76	0.41	9.19	2.03
#95		0.24	32.68	8.2	7.48	0.76	0.4	9.29	2.05
#100		0.24	33.64	8.21	7.6	0.76	0.4	9.19	2.03
#101		0.36	36.06	8.18	7.48	0.76	0.41	9.26	2.05
MARTHA'S VINEYARD									
Martha Son3D	2001-2008	0.12	24.65	6.53	6.13	0.7	0.46	6.89	2.15
	(missing data 2005-2008)								
WEATHER FLOW									
Point Judith	2005-2007	0.04	24.96	7.06	6.51	0.82	0.79	7.98	2.02
Rose Island	2005-2007	0.025	25.04	6.39	6.03	0.69	0.58	7.17	1.82
Halfway Rock	2005-2007	0.03	25.69	6.56	6.15	0.69	0.6	5.98	1.82
Buzzard Bay									
BUZM3	1999	0.01	26.6	8.3	7.94	0.52	0.14	9.36	2.14
	1999-2007	0.01	32.81	8.5	8.15	0.59	0.36	9.58	2.19

Table 3 Sensitivity of mean value at 65 m to assumption of friction coefficient

Roughness coefficient alpha = 0.1 or alpha=1/7
Criteria Choice of roughness coefficient : identical to ATM to compare with Buzzard Bay data

Station WIS	Period	Simulation height	Mean @	Mean @ m/s r=1	Mean @ m/s r=0.	Mean @ m/s r=0	Mean @ m/s r=1/	Mean @ r=0.1	Mean @80 m m/s r=1/7
#74	1980-19	10 m	6.83	7.77	7.48	8.23	8.92	8.41	9.19
#75		simulated	6.80	7.74	7.44	8.20	8.88	8.37	9.15
#76		data				8.16		8.33	
#77						8.13		8.30	
#78						8.12		8.29	
#79						8.12		8.29	
#89						8.15		8.32	
#95						8.20		8.37	
#100						8.21		8.38	
#101						8.18		8.35	

Station	Period	Anemo height (	U (m/s at Hre	Mean @ r=1/7	Mean @ m/s r=1	Mean @ m/s r=0.	Mean @ m/s r=0	Mean @ m/s r=1/	Mean @ r=0.1	Mean @80 m m/s r=1/7
MARTHA VINEYARD										
Martha	2001-20(	12.5 m	5.54	5.37	6.11	5.93	6.53	7.01	6.67	7.22
WEATHER FLOW										
Point Ju	2005-20(	22.25 m	6.34	5.65	6.44	6.41	7.06	7.39	7.20	7.61
Rose Is.	2005-20(	10.66 m	5.34	5.29	6.02	5.81	6.39	6.91	6.53	7.12
Halfway	2005-20(	8.23 m	5.33	5.48	6.24	5.95	6.56	7.16	6.69	7.38
NOAA station										
Buzzarc	1999	24.8 m	7.53		7.53		8.30	8.66		
	1999-20(	24.8 M	7.72	6.80	7.72		8.50	8.86	8.68	9.10

Table 4 Extreme wind analysis for 20, 50, 75 and 100 yr return periods at WIS 101

Calculations based on Gumbel distribution fit through monthly maximum data**.** Directions assume meteorological convention 2 sets of extreme events: average value and upper limit of the 95 % confidence interval.

	U(m/s)	U 95 % (m/s)		U(m/s)	U 95 % (m/s)
	Direction 90			**Direction 180**	
100	31	34	100	28	30.4
75	30.1	33	75	27.3	29.6
50	28.9	31.6	50	26.3	28.5
20	26.1	28.4	20	24	25.9
	Direction 120			**Direction 210**	
100	29.7	32.5	100	29.2	31.7
75	28.8	31.5	75	28.5	30.9
50	27.6	30.2	50	27.5	29.7
20	25	27.1	20	25.1	27
	Direction 150			**Direction 240**	
100	27.8	30.3	100	31.3	34
75	27	29.4	75	30.5	33.1
50	26	28.2	50	29.3	31.8
20	23.6	25.6	20	26.7	28.9

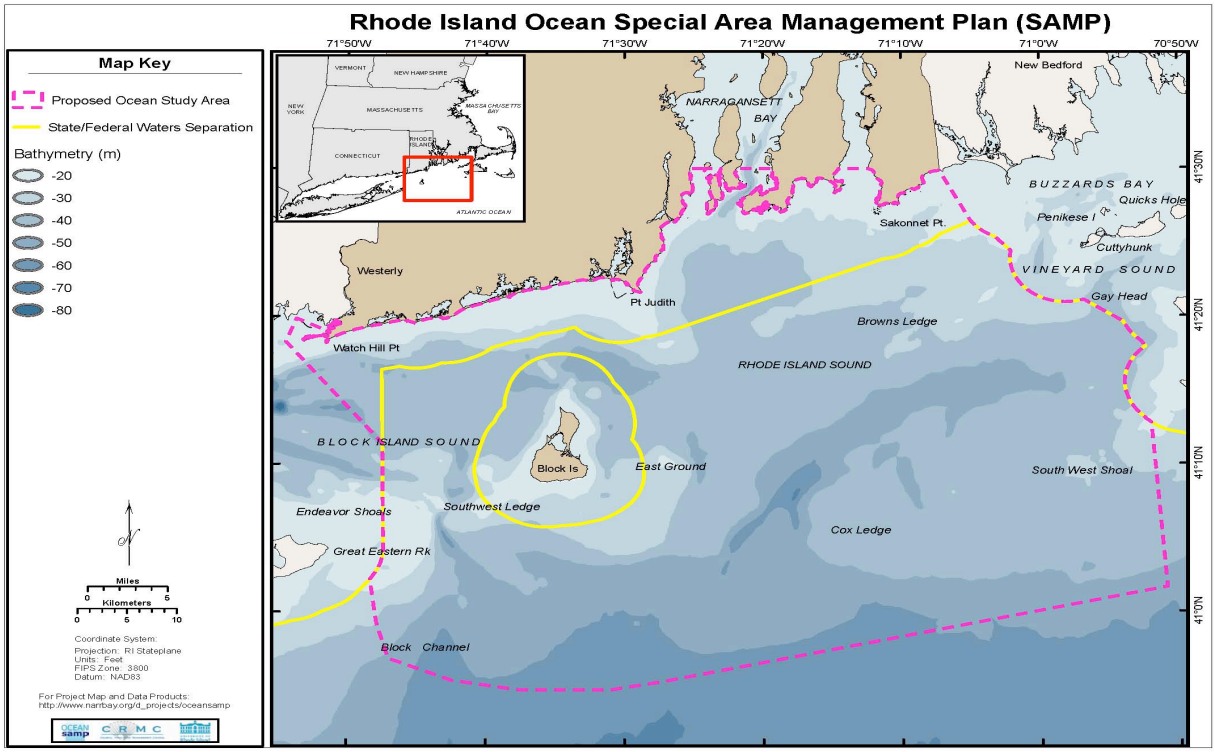

Figure 1 RI Ocean SAMP coastal study area. The dashed line is the study area boundary and the solid yellow line is the boundary of state waters. Key location names are provided as well.

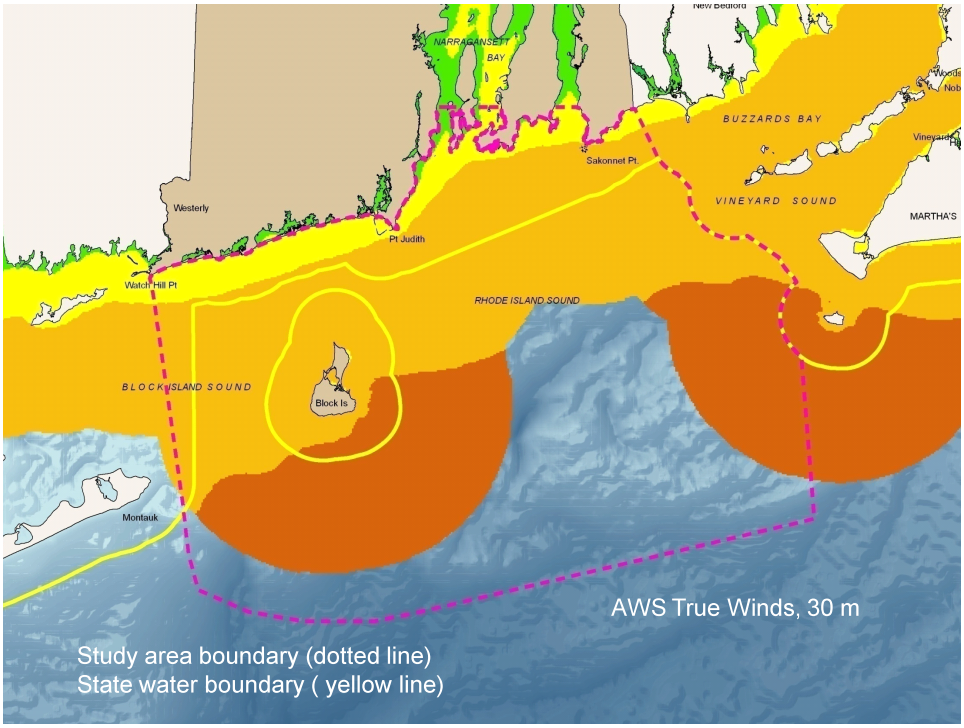

Figure 2a AWS TrueWinds mean annual wind speed at 30 m above sea level

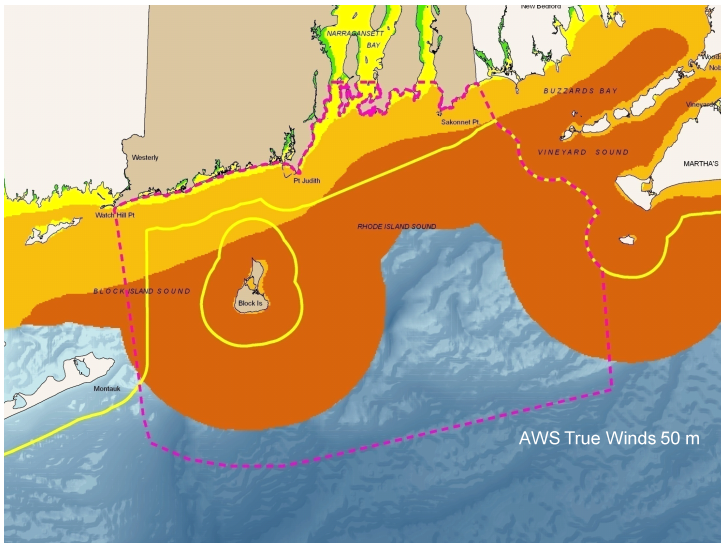

Figure 2b AWS TrueWinds mean annual wind speed at 50 m above sea level.

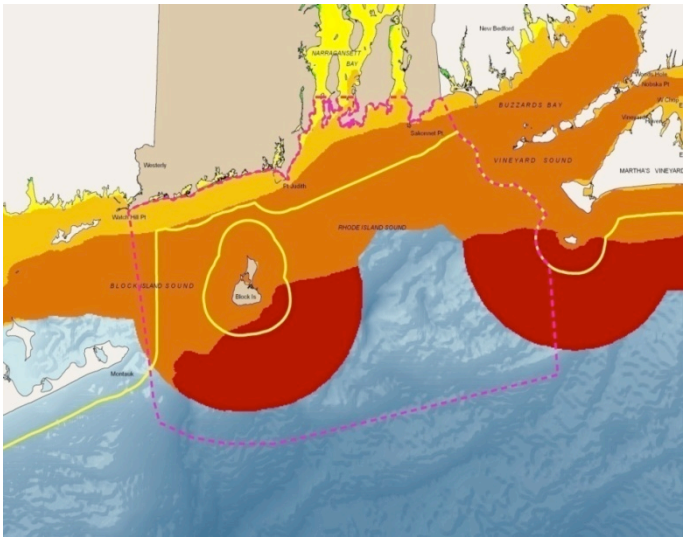

Figure 2c AWS TrueWinds mean annual wind speed at 70 m above sea level.

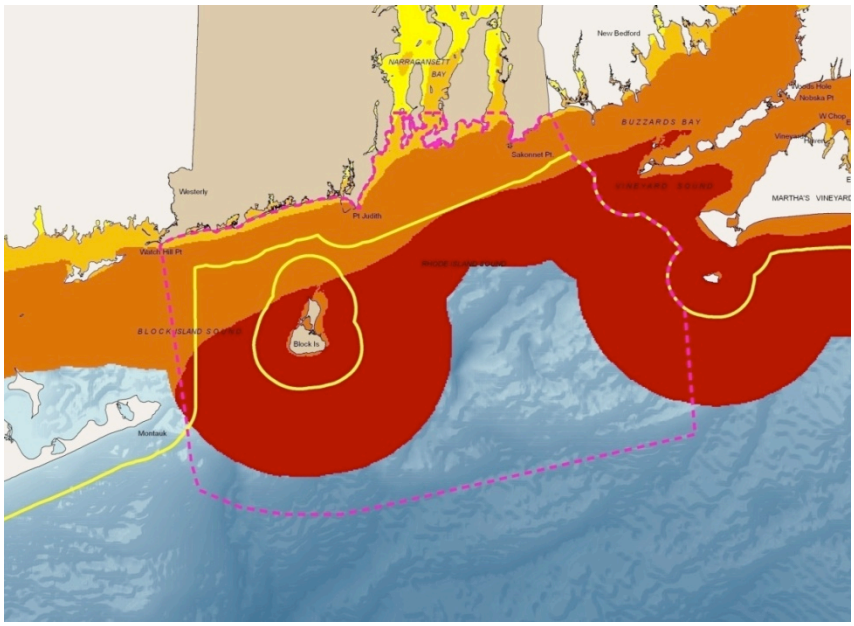

Figure 2d AWS TrueWinds mean annual wind speed at 100 m above sea level.

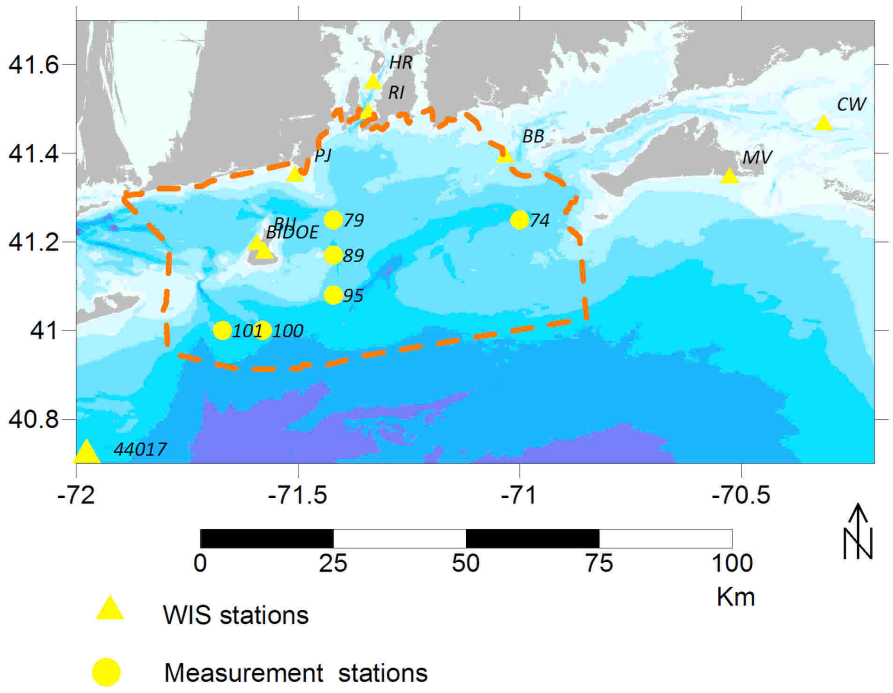

Figure 3 Location of U.S. Army corps of Engineer WIS stations and all measurement stations , Point Judith(PJ), Half Way Rock(HR), Buzzard Bay (BB), Martha's Vineyard (MV), Cape Wind(CW),Block Island Jetty(BIJ), Block Island DOE (DOE), NOAA 44017 (44017) (Cape Wind is not used in the analysis for reasons of confidentiality).

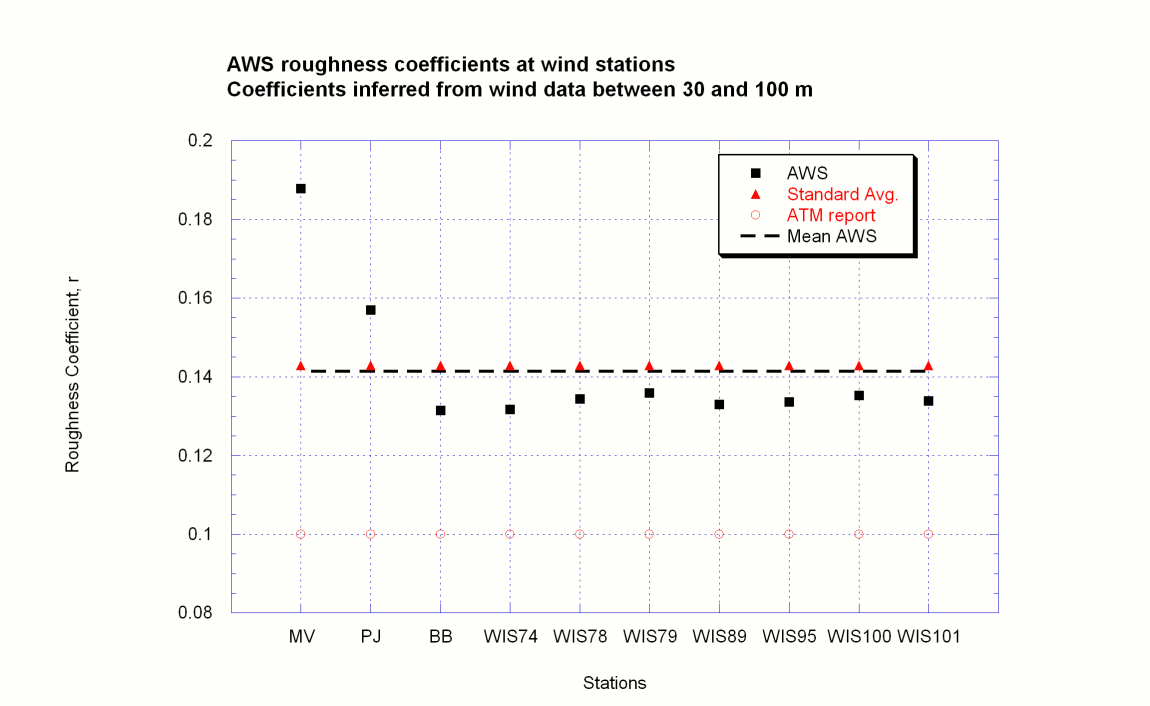

Figure 4 Friction coefficient for each observation station based on the AWS data, standard average value and the value assumed by ATM (2007a). The mean AWS value is also presented.

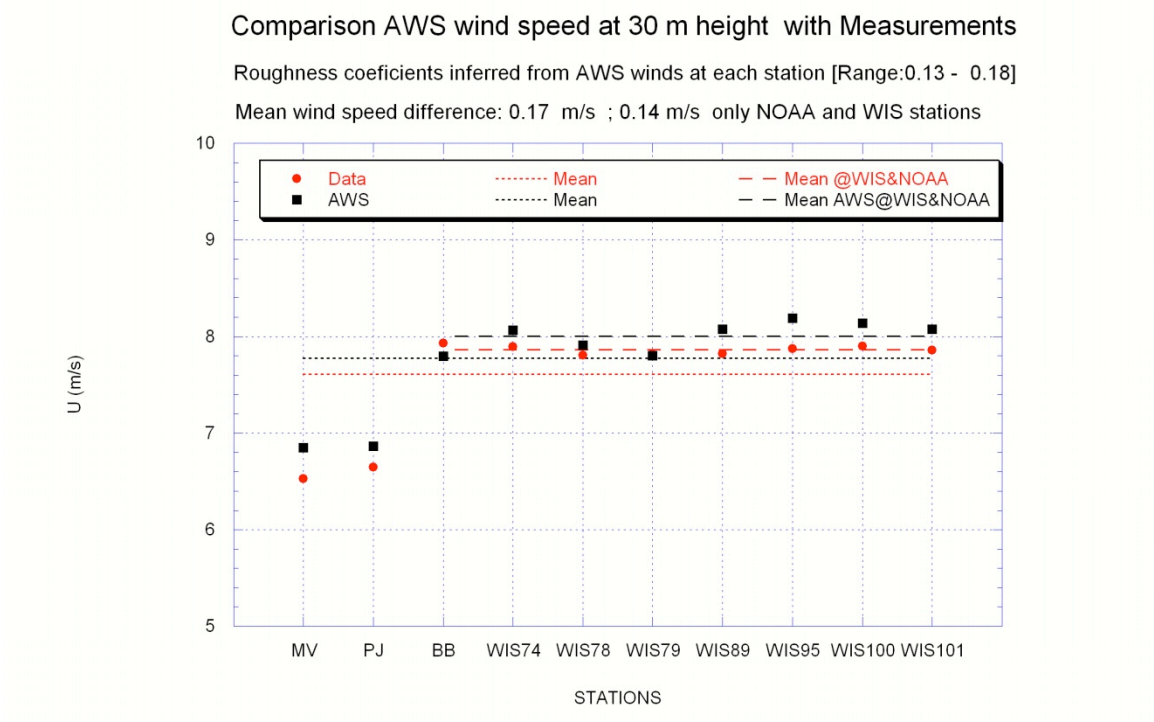

Figure 5 Comparison of the mean wind speed at each observation station with AWS True Winds data at an elevation of 30 m. The mean values for WIS and NOAA sites are also shown.

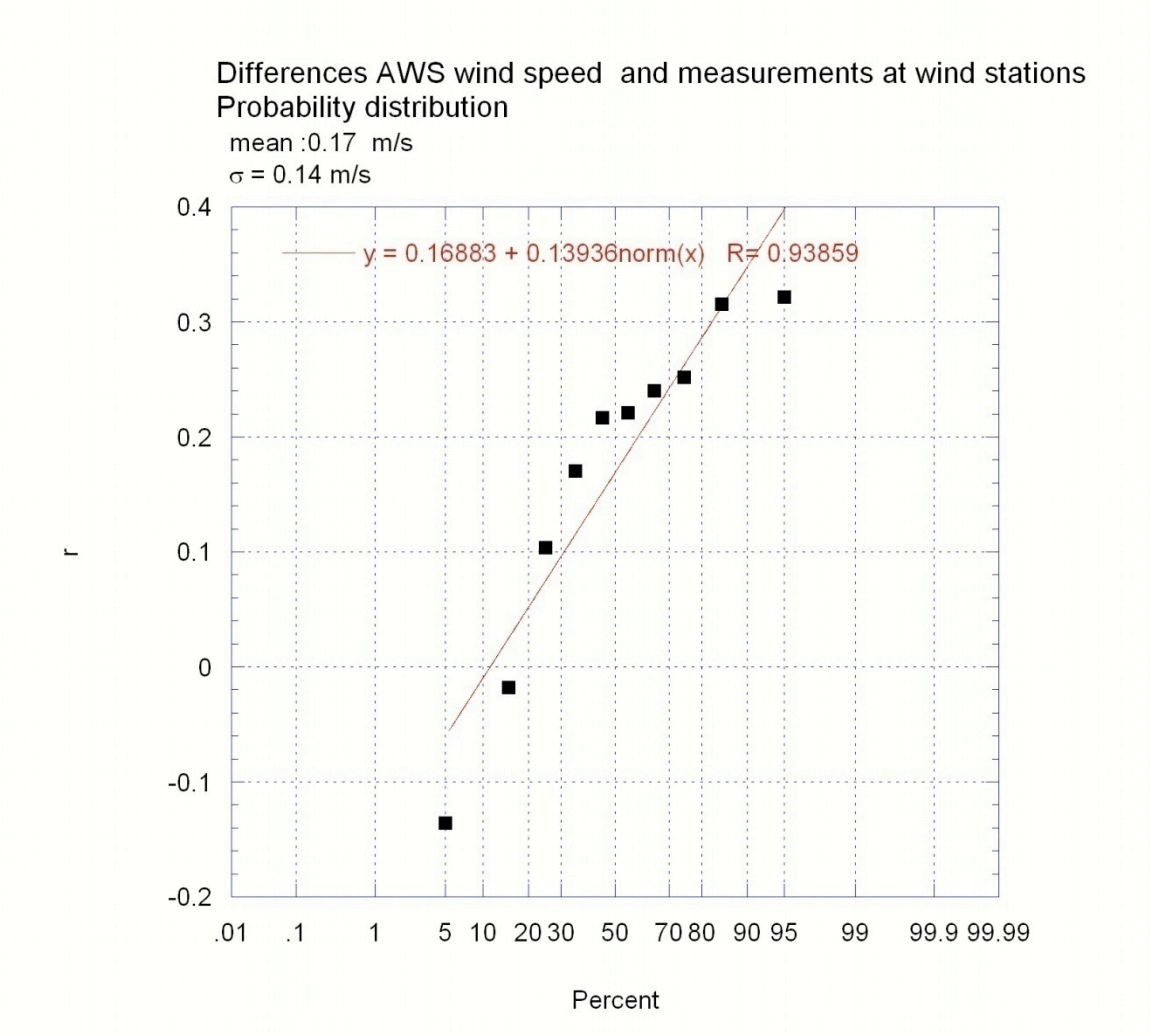

Figure 6 Probability distribution of the difference between observed and computed wind speeds at the selection observation locations at 30 m. A normal distribution curve fit to the difference data is shown.

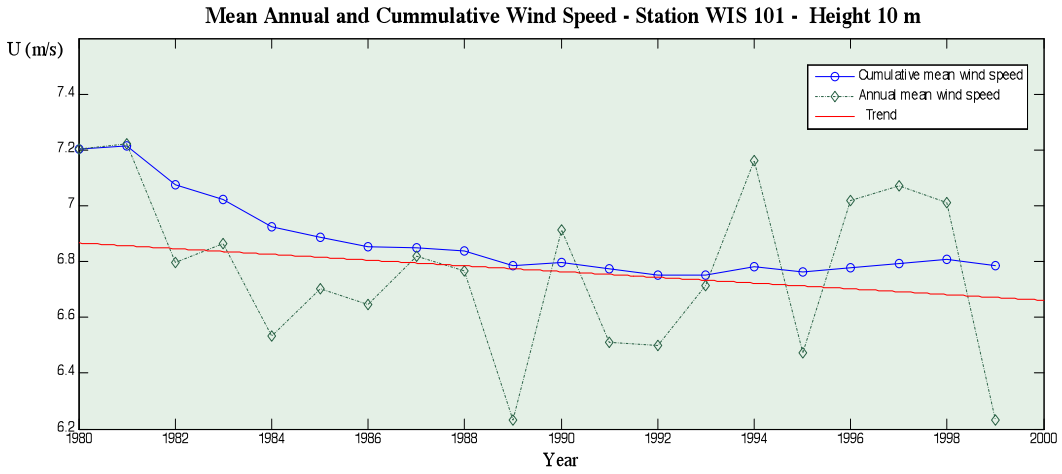

Figure 7 Mean annual and cumulative wind speed at WIS 101 versus time (1980-1999) at 10 m elevation. The trend line is also shown.

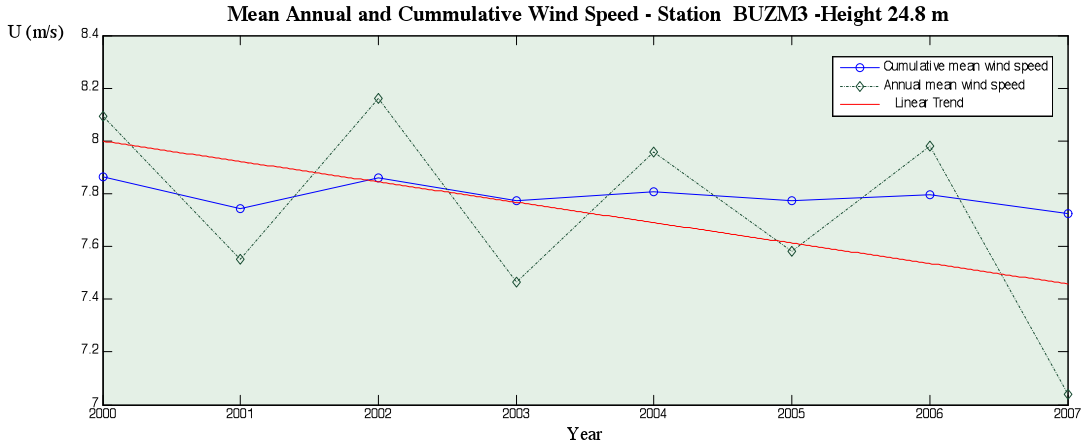

Figure 8 Mean annual and cumulative wind speed at BUZM3 versus time (2000- 2007) at 24.8 m elevation. The trend line is also shown.

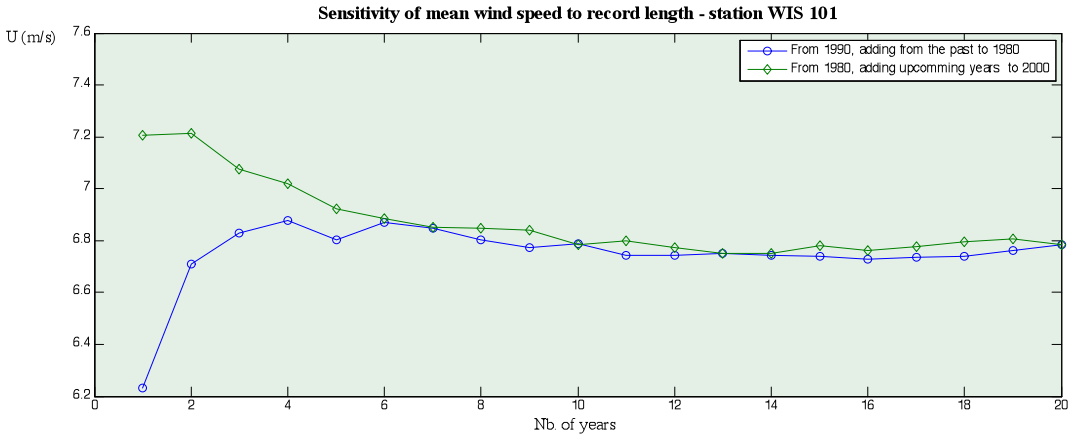

Figure 9 Cumulative mean wind speed versus number of years for both forward and backward averaging at WIS 101, 10 m elevation.

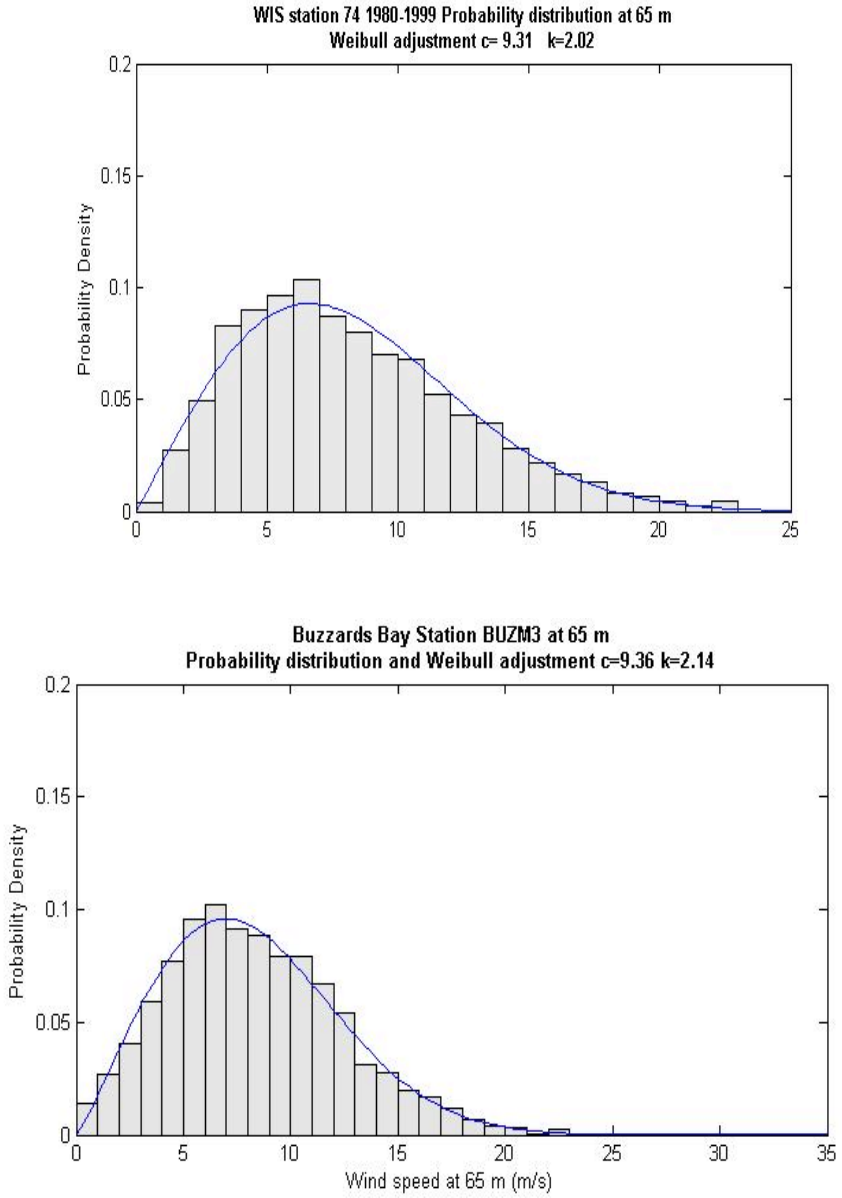

Figure 10 Probability distribution of wind speed at 65 m for WIS 74(upper panel) and BUZM3 (lower panel) stations. The solid line represents a least squares, Weibull distribution fit to the data, with the c and k values given in the header.

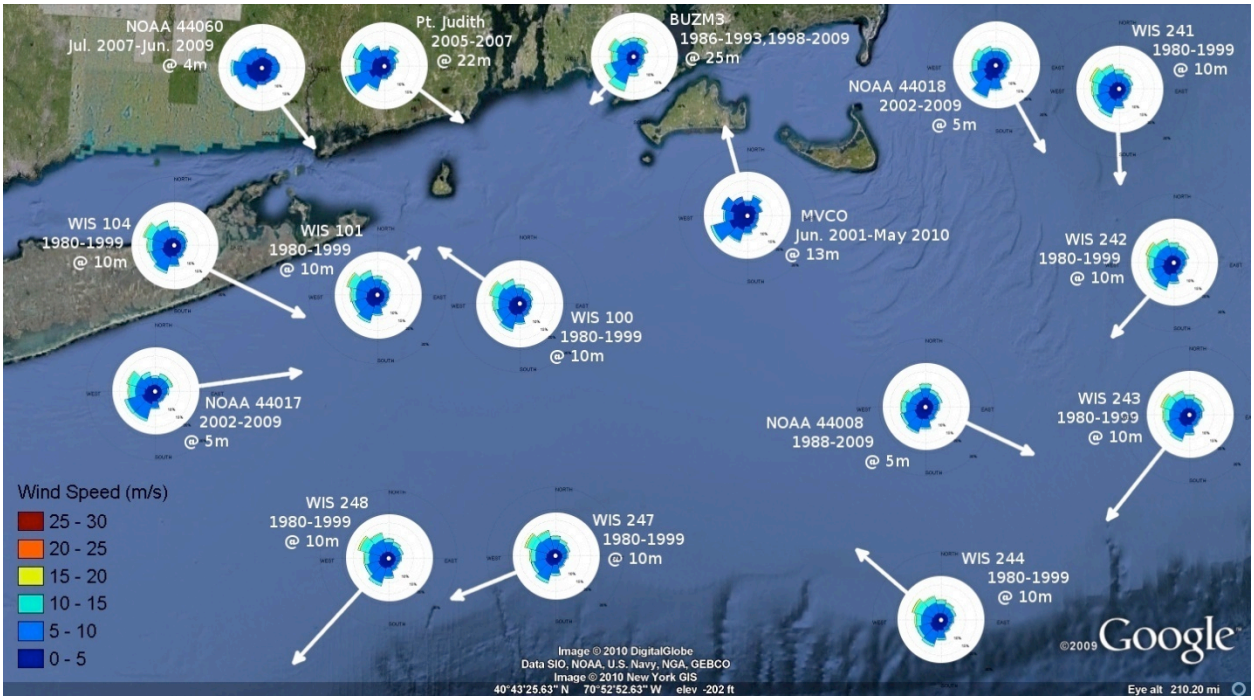

Figure 11 Wind speed frequency roses for SAMP study area.

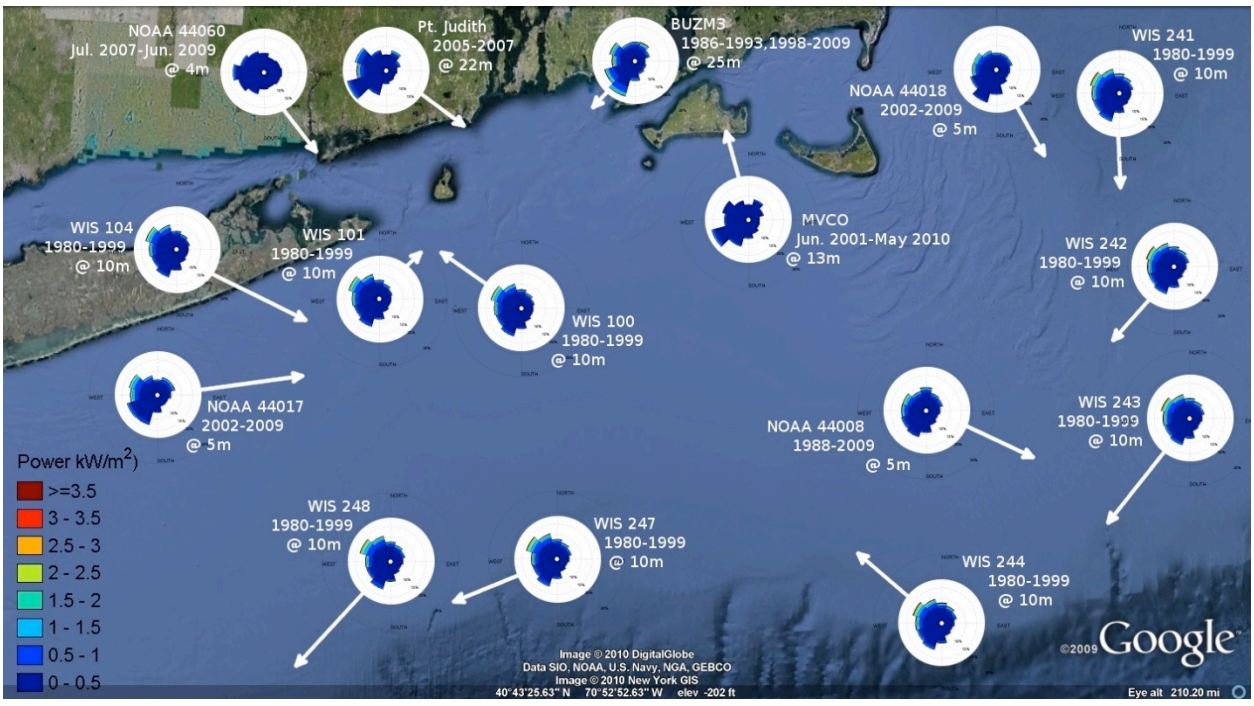

Figure 12 Wind power roses for SAMP study area.

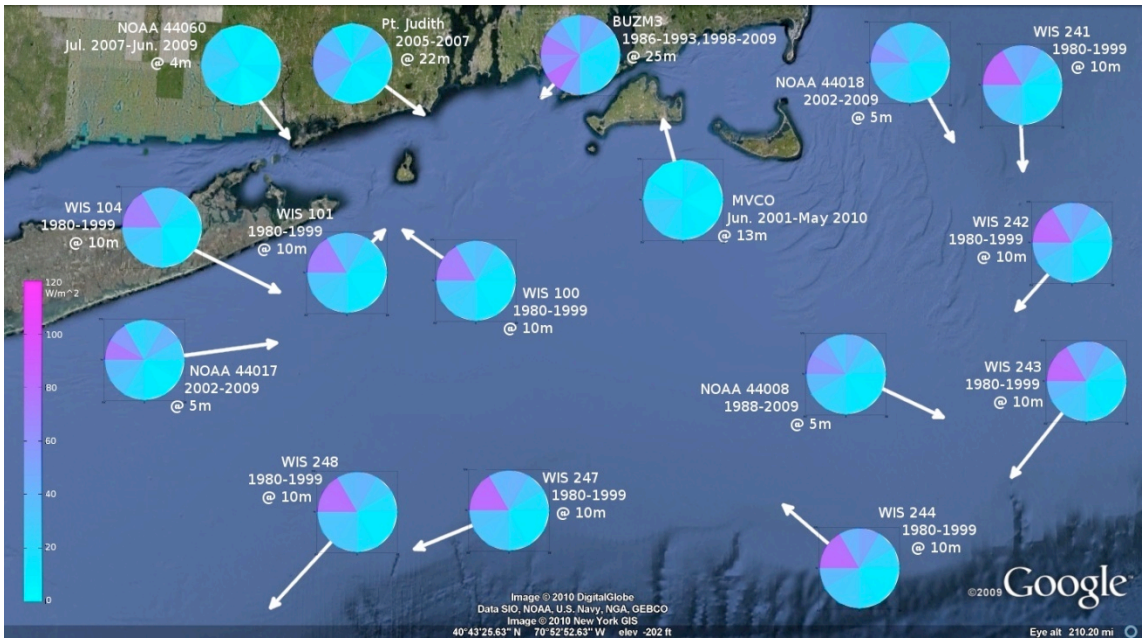

Figure 13 Mean wind power rose for SAMP study area.

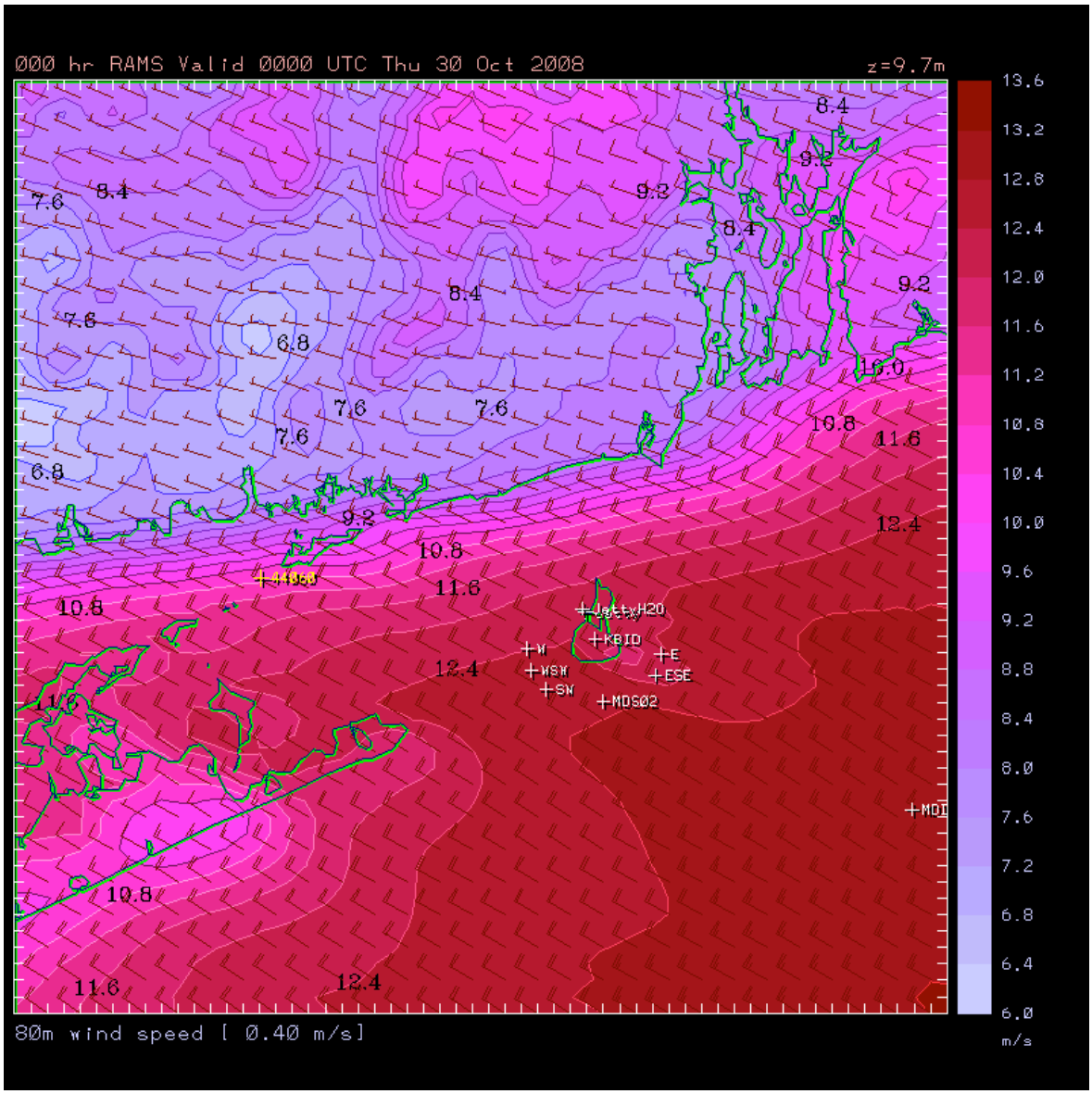

Figure 14 RAMS meteorological model predicted wind field in SAMP study area on October 30, 2008 (NW case).

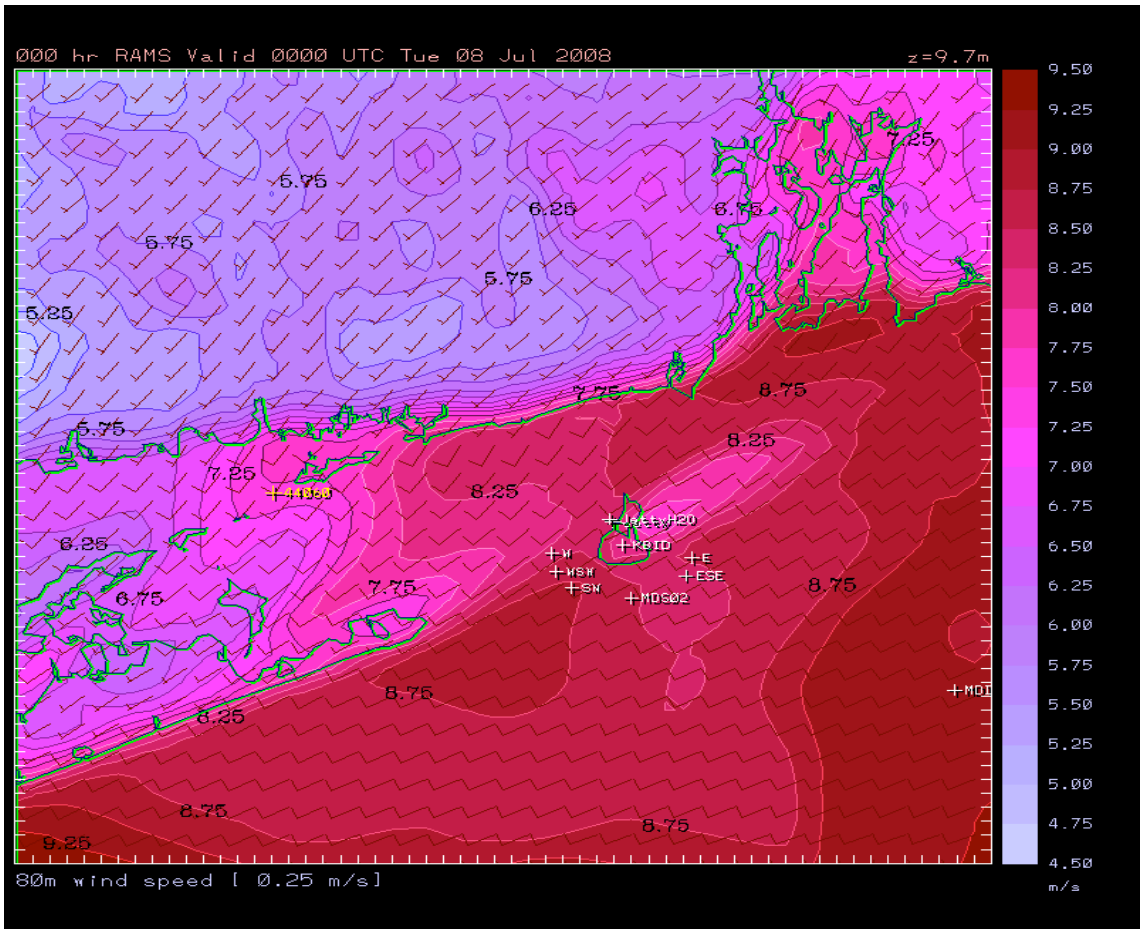

Figure 15 RAMS meteorological model predicted wind field in SAMP study area on July 8, 2008 (SW case).

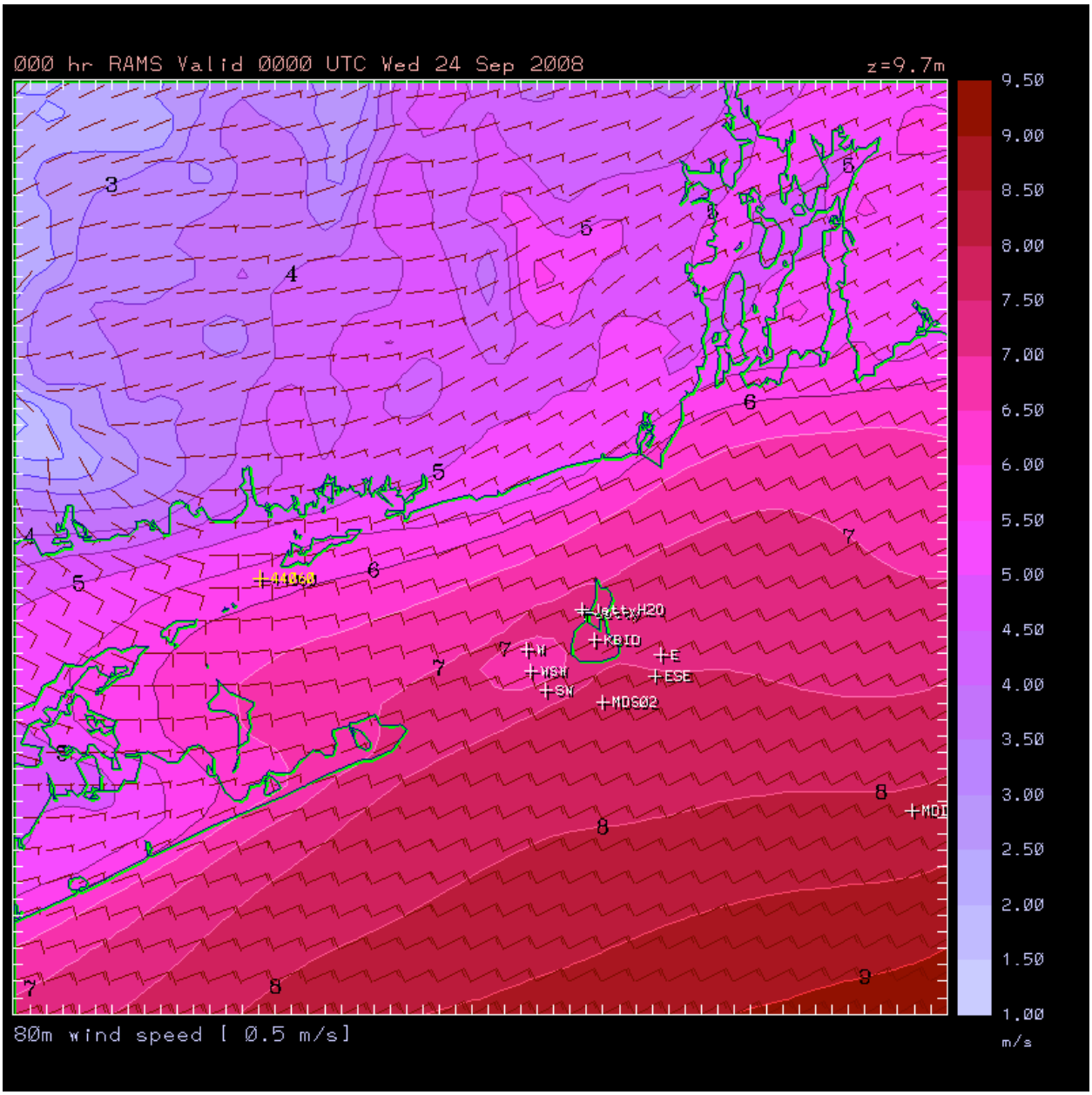

Figure 16 RAMS meteorological model predicted wind field in SAMP study area on September 24, 2008.

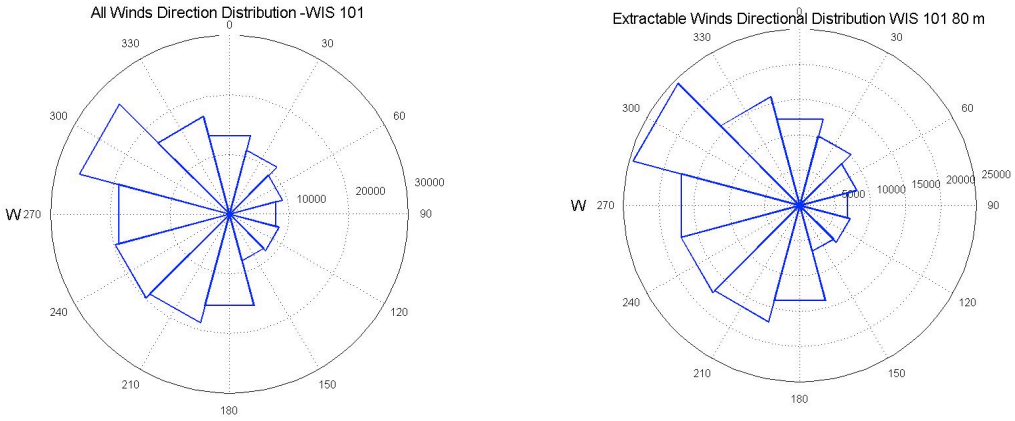

Figure 17 Wind directional distribution by count at 80 m elevation for WIS 101 (1980-1999, hourly data). Left panel includes all wind data and right panel extractable winds (3.5 to 27 m/sec). (Note difference in scale.)

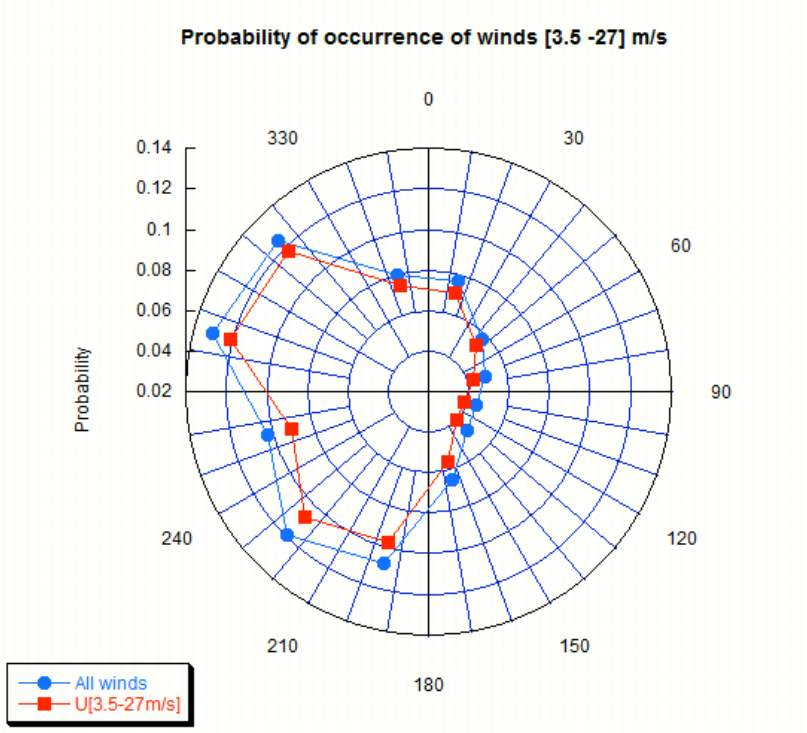

Figure 18 Probability of occurrence by direction for all and extractable winds at WIS101, 80 m elevation.

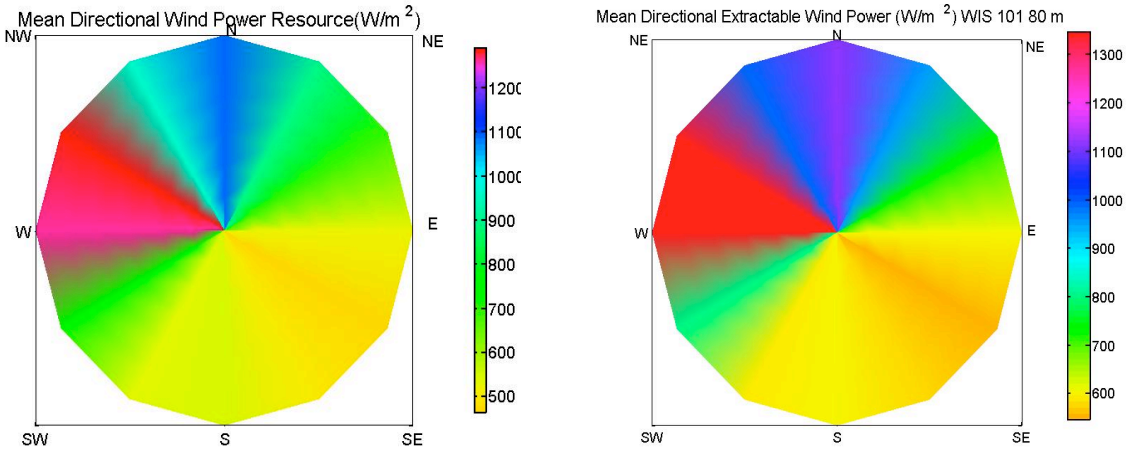

Figure 19 Mean directional wind power resource, all (left panel) and extractable (right panel).

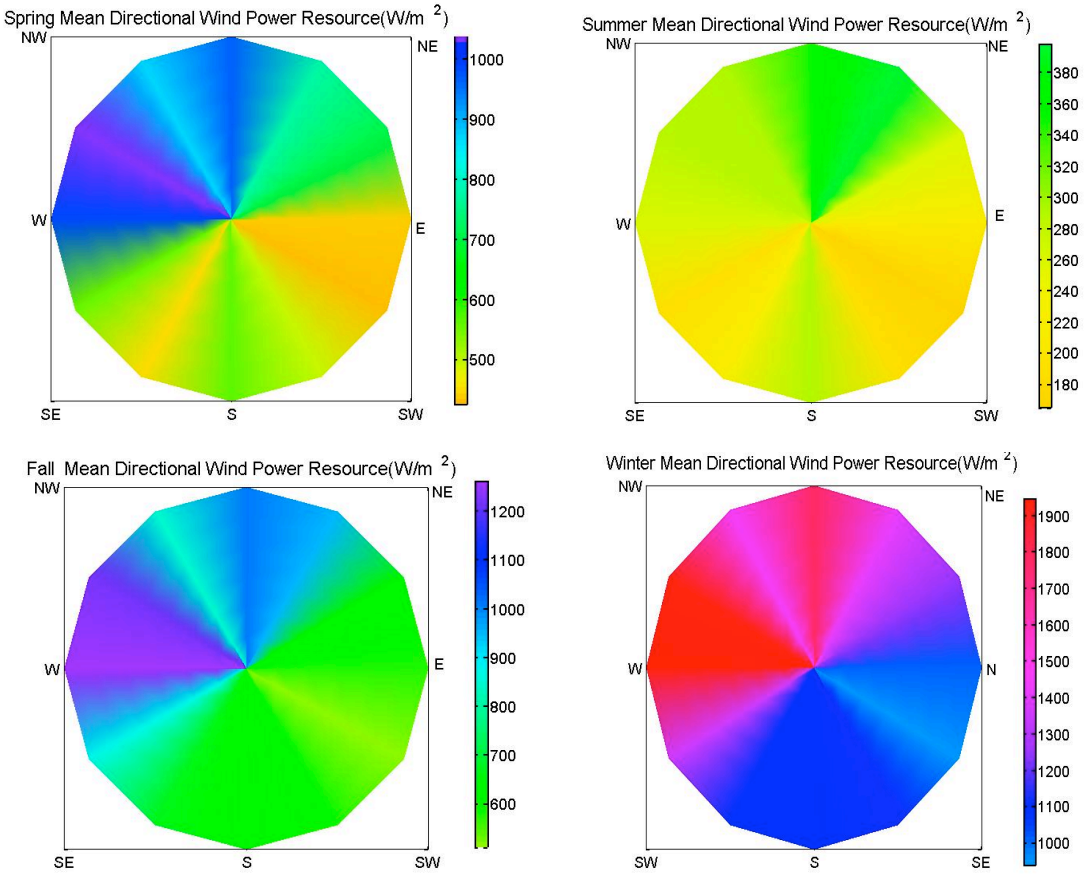

Figure 20 Mean wind power resource by direction for each season of the year, spring, summer (upper panel, left and right) and fall, winter (lower panel, left and right).

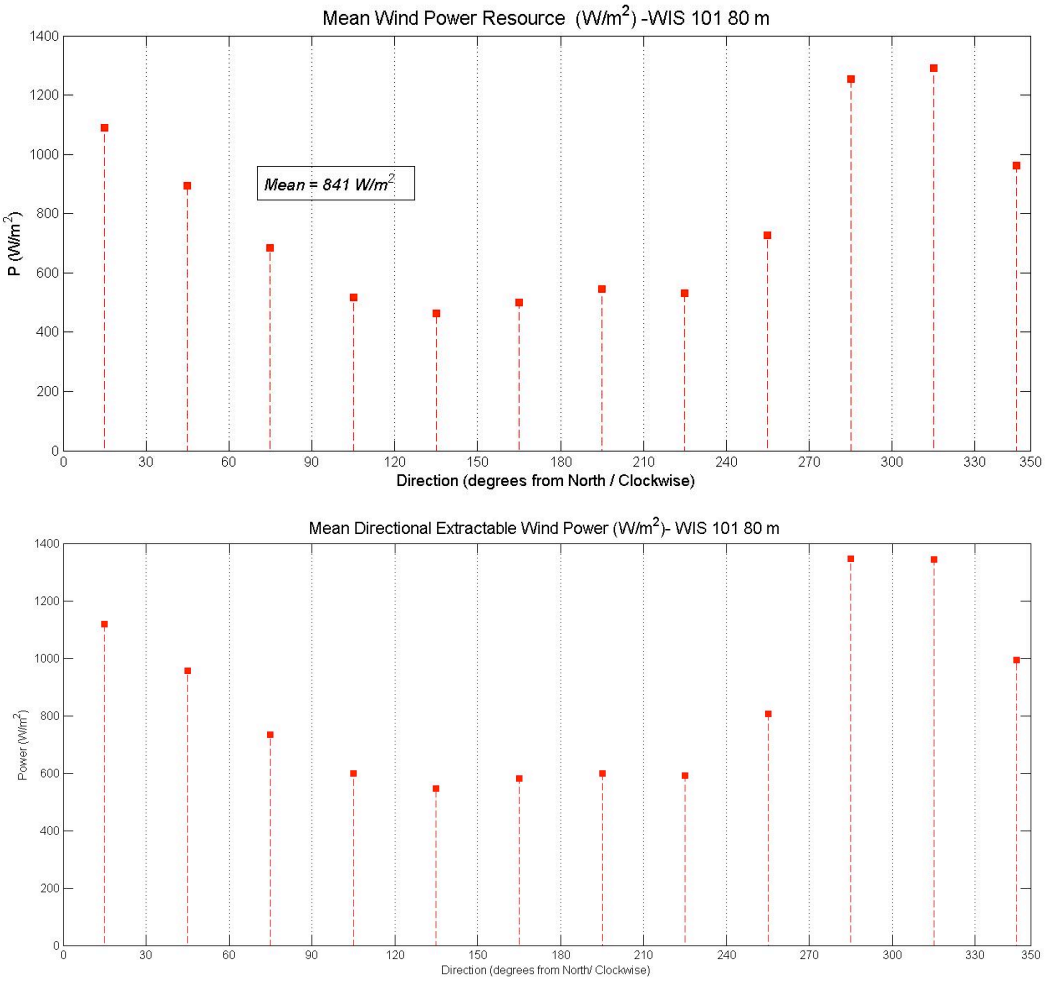

Figure 21a Mean wind power all (upper panel) and extractable (lower panel) by direction, WIS 101, 80 m.

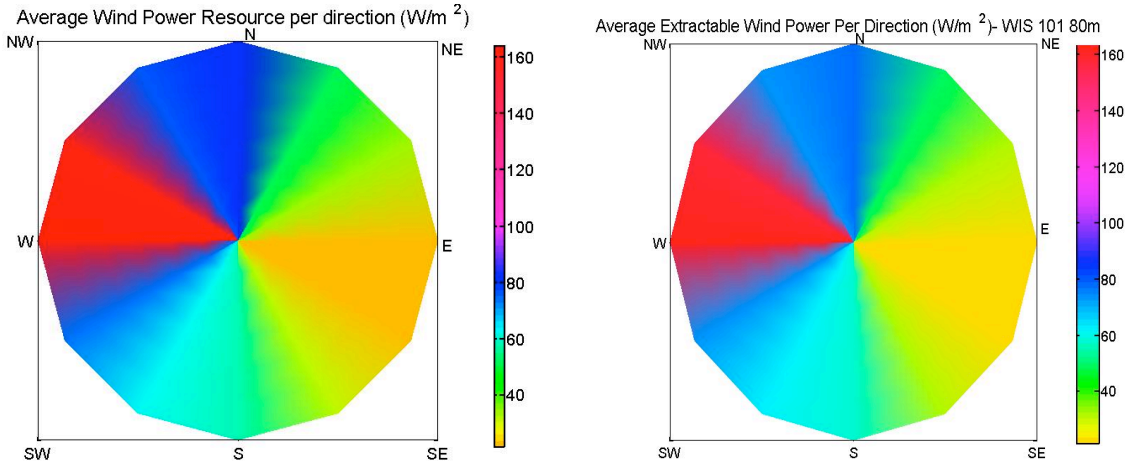

Figure 21b Average wind power resource by direction, total (left panel) and extractable (right panel), WIS 101, 80 m.

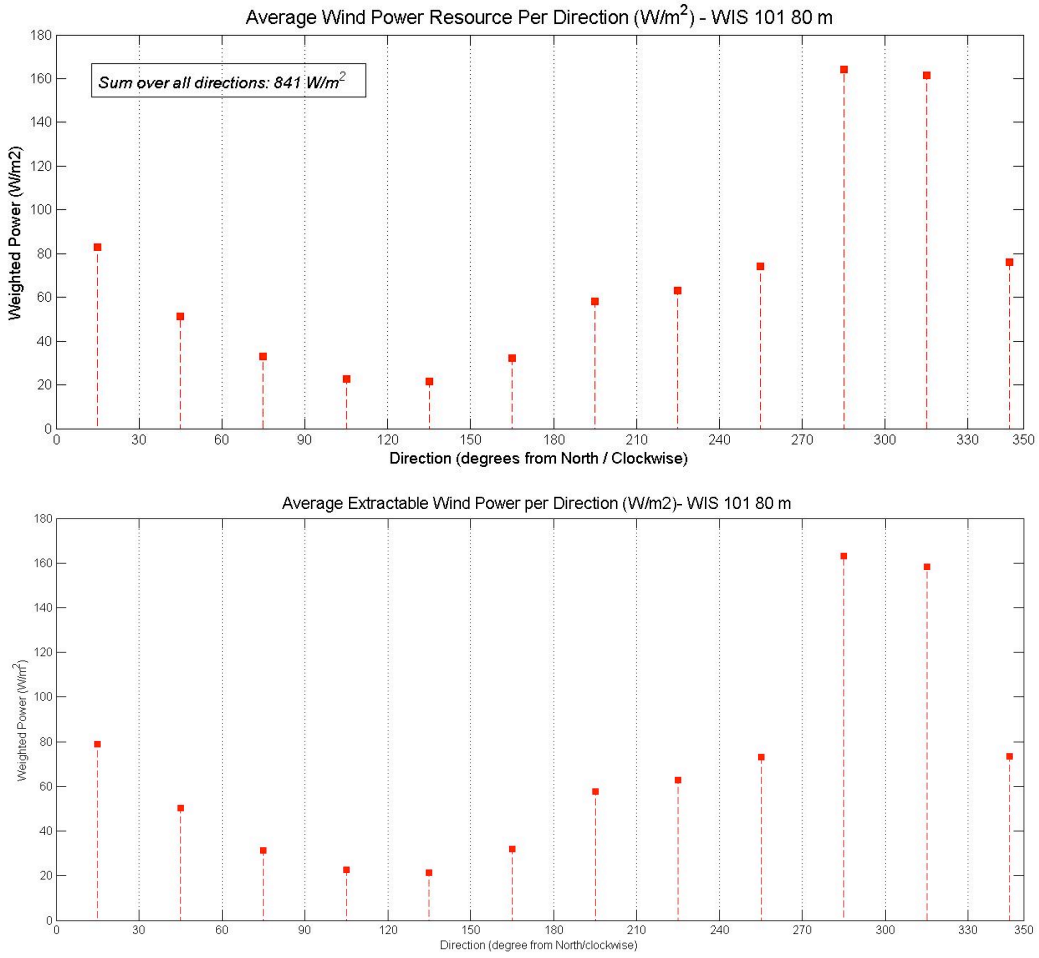

Figure 22 Average wind power by direction, all winds (upper panel) and extractable winds (lower panel), WIS 101, 80 m.

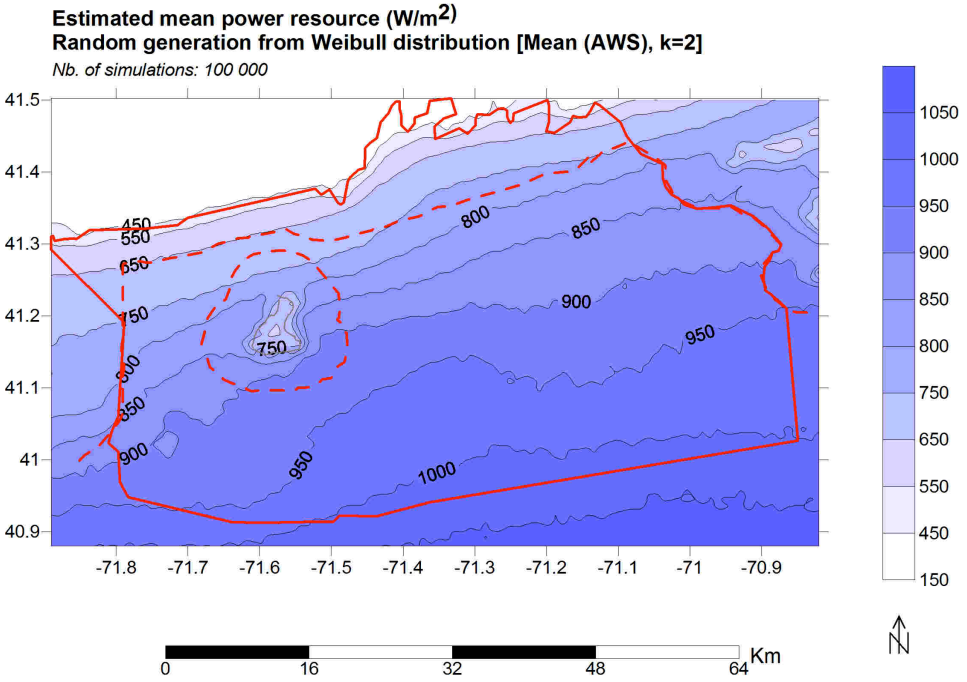

Figure 23 Contours of mean wind power in the study area based on AWS all winds.

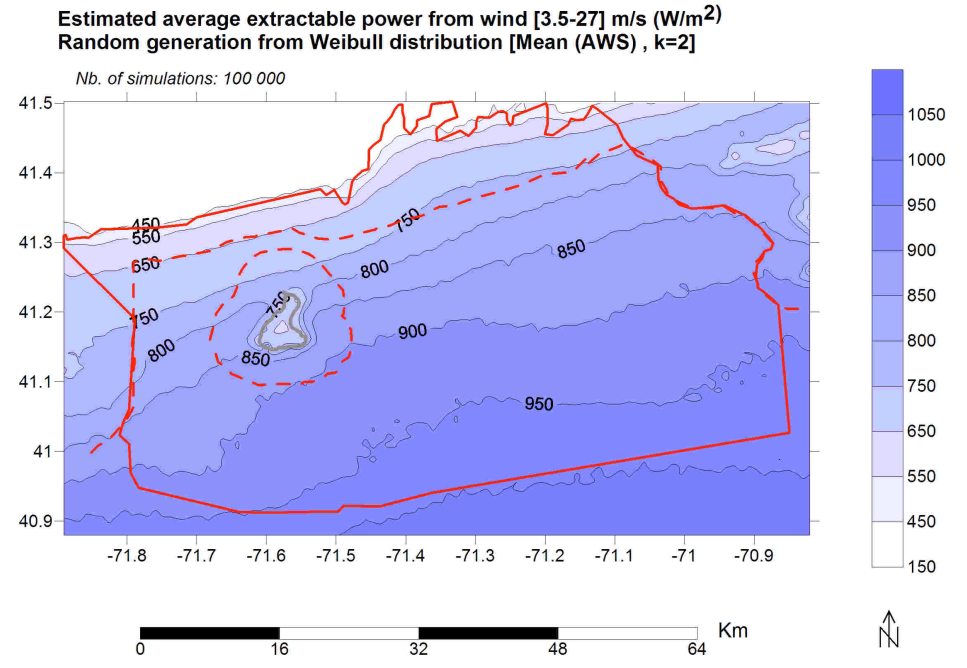

Figure 24 Contours of mean wind power in the study area based on AWS extractable winds.

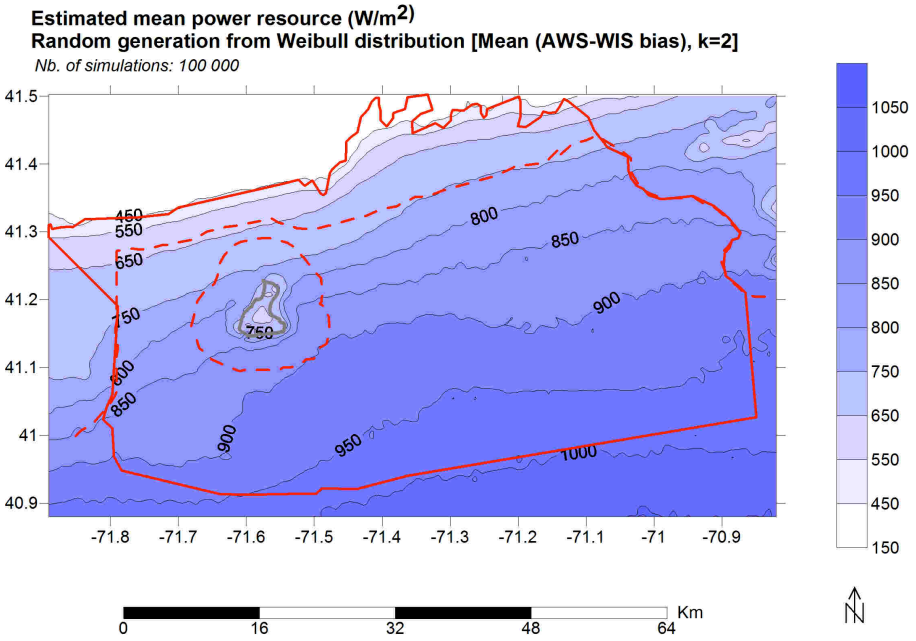

Figure 25 Contours of mean wind power in the study area based on AWS minus bias, all winds.

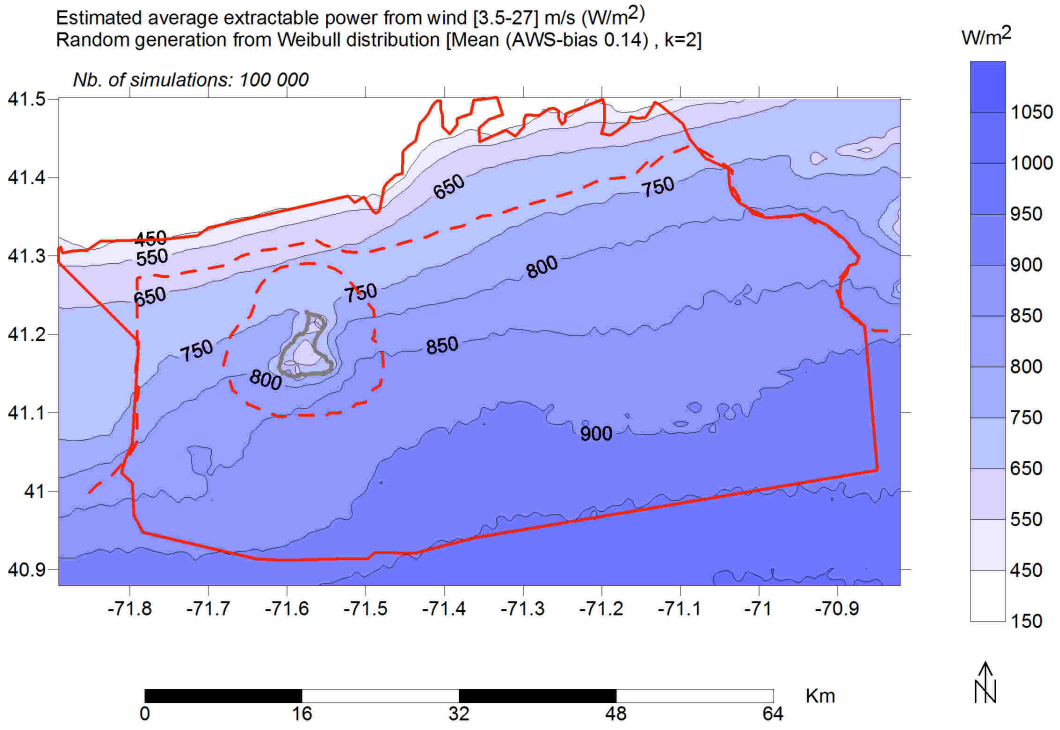

Figure 26 Contours of mean wind power in the study area based on AWS minus bias, extractable winds.

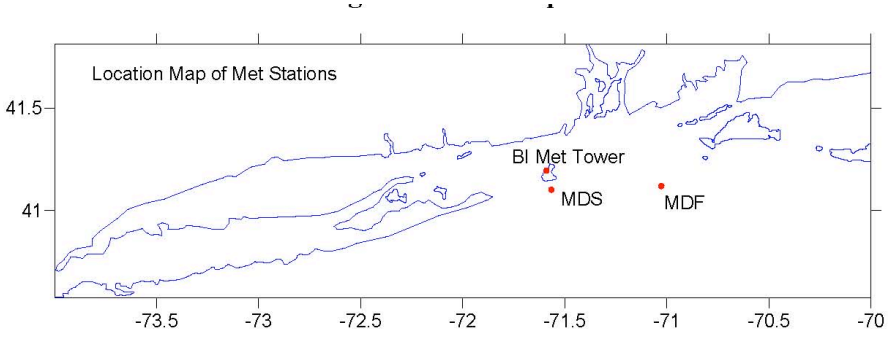

Figure 27 Location map for MDS, MDF and AWS Met tower.

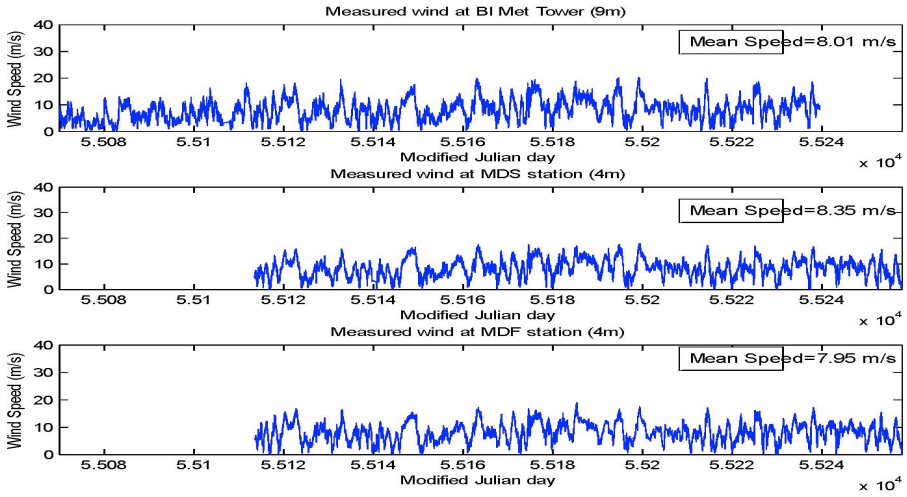

Figure 28 Wind time series at AWS Met, MDS, and MDF, from beginning of record to February 1, 2010.

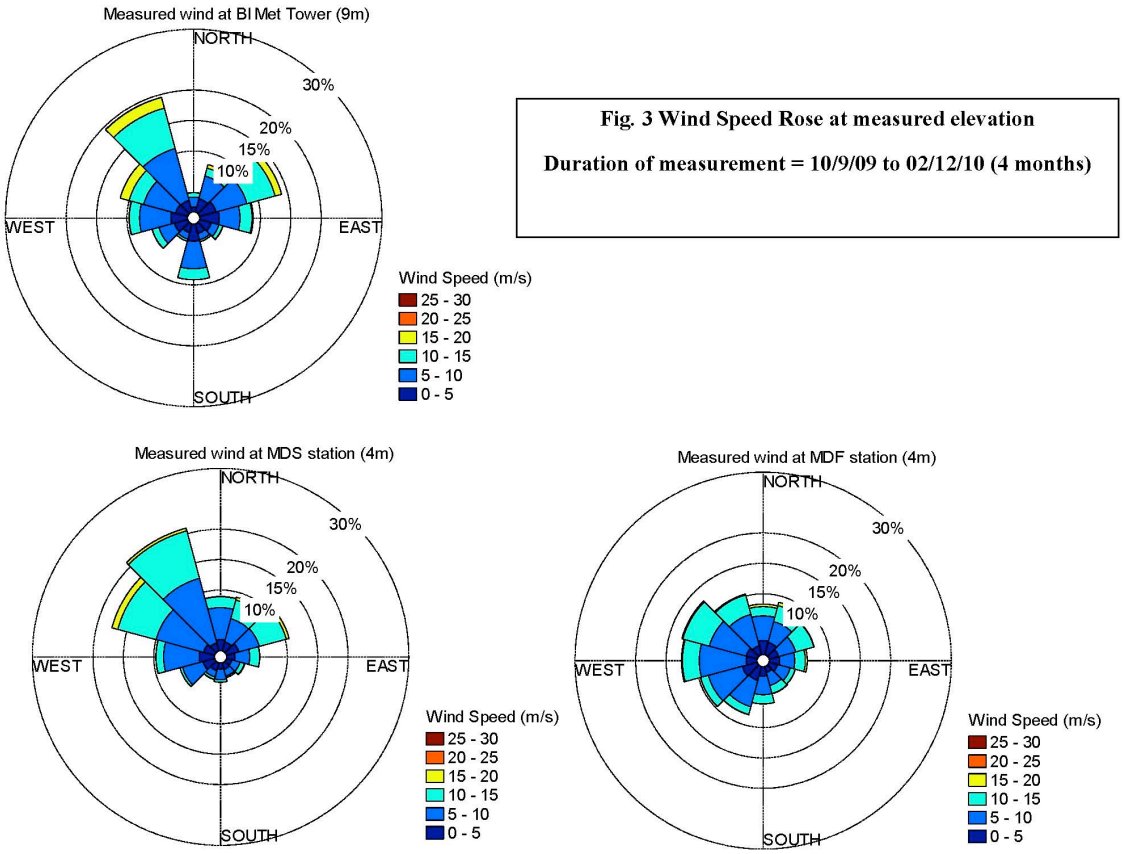

Fig. 3 Wind Speed Rose at measured elevation

Duration of measurement = 10/9/09 to 02/12/10 (4 months)

Figure 29 Wind speed rose for AWS Met, MDS, and MDF from October 9, 2009 to February 12, 2010.

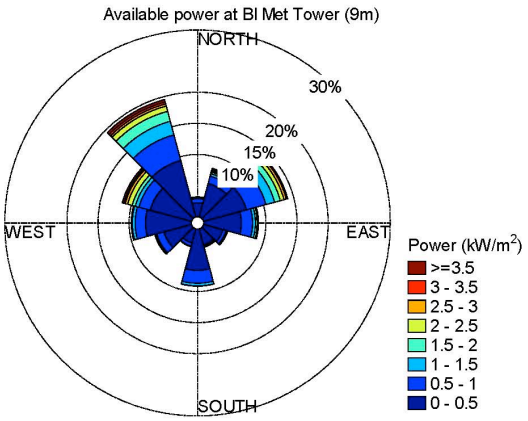

Fig. 4 Wind Power Rose at measured elevation

Duration of measurement = 10/9/09 to 02/12/10 (4 months)

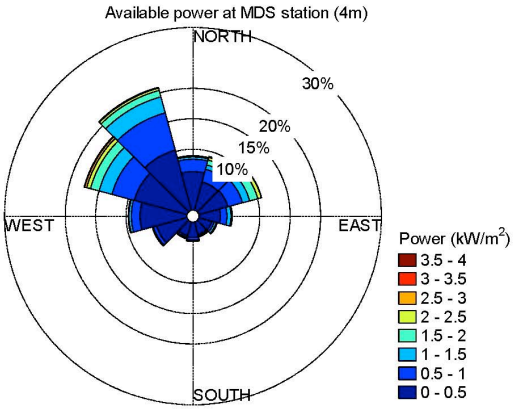

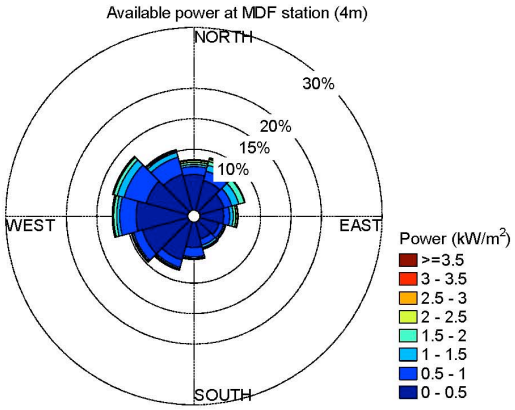

Figure 30 Wind power rose for AWS Met, MDS, and MDF from October 9, 2009 to February 12, 2010.

Appendix A

Wind frequency and power density (seasonal and annual) roses and Weibull distribution fits for selected stations in the SAMP study area.

For this appendix material, see Appendix A of Spaulding, et al., 2010, "Wind Resource Assesment in the Vicinity of a Small, Low Relief Coastal Island" – this report.